

USING PETROLOGY AND MINERALOGY TO UNDERSTAND THE SURFACE OF VESTA: A
COLLECTION OF FINE-GRAINED EUCRITES

by

SAMANTHA ELIZABETH SMITH

Bachelor of Science, 2009
Texas A&M University-Corpus Christi
Corpus Christi, TX

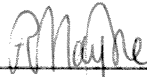
Submitted to the Graduate Faculty of the
College of Science and Engineering
Texas Christian University
in partial fulfillment of the requirements
for the degree of

Master of Science

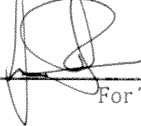
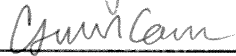
Spring 2012

USING PETROLOGY AND MINERALOGY TO UNDERSTAND THE SURFACE OF VESTA:
A COLLECTION OF FINE-GRAINED EUCRITES

Thesis approved:



Major Professor



For The College of Science and Engineering

Acknowledgements

I was fortunate enough to have many fantastic people to help and support me throughout my thesis and graduate work. Thank you to everyone who has been a part of this journey with me.

First, I would like to thank my advisor, professor Dr. Rhiannon Mayne. I greatly appreciate you sharing your knowledge of meteoritics. You have given me the opportunity to work on a project for my thesis that I really love. Your patience and constant guidance helped make my project as successful and enjoyable as I had hoped it would be.

I would also like to thank everyone that helped me at the Smithsonian, especially Dr. Cari Corrigan, Dr. Emma Bullock and Nicole Lunning. You were all extremely helpful with the SEM and electron microprobe and a joy to work with.

Finally, to my colleagues, friends and family, I could not have done this without you. To Nick Utter, you were very helpful with Photoshop and kept me equilibrated when thesis-ing got too stressful. To my parents, I appreciate that you have always supported me in every direction I've gone in my life and I love you very much.

Table of Contents

Acknowledgements.....	ii
List of Figures	v
List of Tables	vi
Introduction	1
Background.....	2
Asteroids	2
Differentiation of Planetary Bodies.....	3
The Dawn Mission.....	3
HEDs.....	7
Vestoids	9
Competing Models of Formation for Vesta.....	11
Models of Formation: Fractional Crystallization.....	15
Models of Formation: Partial Melting	15
Models of Formation: Magma Ocean	16
Testing Models of Formation for Vesta.....	16
Thermal Metamorphism in Eucrites.....	17
Testing Models for the Formation of Vesta: Using ALH A81001.....	21
Methodology	28
Samples.....	28
SEM Maps.....	28
Electron Microprobe	35
Results.....	37

Texture and Mineralogy	37
Mineral Chemistry.....	40
Equilibration.....	43
MIL 07664,4A description	43
MIL 07664,4B description	44
QUE 99033,2A description.....	46
QUE 99033,2B description	47
QUE 97001 description.....	49
EET 96002 description	50
ALH 090004A description	51
ALH 090004B description	52
Discussion	54
Implications for Vesta and Fine-grained Eucrites Using ALH A81001	54
Comparisons of Samples with Two Clasts	56
Unique Eucrite Clasts.....	58
Reverse Zonation	58
Expanding our Knowledge of Fine-grained Eucrites.....	62
Conclusions.....	63
References.....	66
Vita	
Abstract	

List of Figures

1. Photo of Vesta by the Dawn spacecraft	4
2. Ceres	5
3.a-c Photos of a polymict eucrite, diogenite, and howardite.....	8
4. Spectral data comparing Vesta and the HEDs.....	10
5. Location of Kirkwood gaps	12
6. The 3:1 Kirkwood gap	13
7. The Stannern and Main Group-Nuevo Laredo trends	14
8a-e. Pyroxene equilibration trends for the major elements.....	18
9. Minor pyroxene trends of pyroxene	20
10. BSE image of ALH A81001.....	22
11. Partial melting model	23
12. Magma ocean model.....	25
13a-b. Description of SEM procedure	31
13c. Description of SEM procedure, continued.....	32
14. An example of SEM element maps used to represent minerals when combined	34
15. BSE image of MIL 07664,4B.....	36
16. Microprobe data for pyroxenes in eucrite clasts	41
17a-b. Fe/Mn versus Fe/Mg plot for eucrites.....	42
18. Comparison of Ibitira and QUE 99033,2B	49
19. Dawn at Vesta.....	60
20. MIL 07664,4A pyroxene exhibiting reverse zoning	61

List of Tables

1. Comparison of the formation environment for ALH A81001	26
2. All howardites examined in this study	29
3. Magnification used to analyze SEM mineral maps	30
4. Range of anorthite content present in the plagioclase data	38
5. Degree of equilibration for major and minor elements in pyroxene.....	39

Introduction

The asteroid 4Vesta (the number before the name represents the order in which the asteroids were discovered; hereafter it will be referred to as Vesta) is a planetesimal which offers us an ideal opportunity to understand the processes involved in planetary formation, because it preserves evidence of the processes that occurred early in our Solar System's history. Vesta is the only asteroid with a known associated meteorite group, the howardite-eucrite-diogenite suite (the HEDs), with howardites being a brecciated mixture of eucrites and diogenites. This makes Vesta one of the most studied asteroids, with data from ground-based telescopes, meteorite samples, and the Hubble Space Telescope. Also, new information is returned daily from the NASA Dawn mission, currently orbiting Vesta. However, the formation of Vesta is still not well understood.

Several models have been proposed for the formation of Vesta. The partial melting model and the magma ocean model are the most popular; however, neither can fully explain the geochemical relationships between the HEDs. Recent work by Mayne et al. (2010) on ALH A81001, a quench-textured, unequilibrated eucrite, suggests that this sample and those similar to it may help us test between the two models for Vesta's formation. Eucrites like ALH A81001 are not common (Stolper, 1977; Russell et al., 2004; Mayne et al., 2010). In this regard, howardites (the most abundant member of the HED family) are important because they can contain unique, fine-grained eucrite clasts not found in eucrite-only samples.

This study focuses on finding eucrite clasts, similar to ALH A81001 in the howardite collection, determining their mineralogy and petrology, and comparing them

to previously collected data for the eucrite collection as a whole. This unique group of fine-grained eucrites can provide us with valuable insight into the petrogenesis of Vesta. They will also help us determine variety of the geology that existed on Vesta's surface and within its upper crust shortly after its formation, before it was brecciated and affected by impacts.

Background

Asteroids

Over 99.8% of meteorites are believed to originate from the main asteroid belt between Mars and Jupiter (NASA, 2009). Asteroids are a vital tool for understanding the early history of our Solar System and the formation of planetary bodies, such as Earth. There are two main groups of asteroids: primitive and differentiated. Primitive, undifferentiated asteroids have not experienced melting since their formation and, therefore, they preserve the first materials to crystallize in our Solar System. In contrast, differentiated asteroids have undergone a global-scale melting event, which resulted in a core, mantle, and crust structure.

Studying the meteorites that originate from asteroids is very important for our understanding of our own planet. Meteorites can take us to places that we cannot physically go to on Earth, such as the core. Iron meteorites are samples of cores from asteroids that have been completely disrupted by impacts. Earth is a very geologically active planet, but the asteroids have remained relatively unaltered since their initial formation. All asteroidal meteorites are around a half billion years older than any rock

found on Earth to date. As a result, meteorites can tell us not only what Earth may have looked like before it differentiated, but also how it differentiated.

Differentiation of Planetary Bodies

As previously discussed, the undifferentiated, primitive asteroids are thought to have been the earliest formed materials in the Solar System, while differentiated asteroids have been subject to a heating event after their initial formation. The heat source for differentiated asteroids is from the decay of short-lived radionuclides like ^{26}Al , which decays to ^{26}Mg . These radioactive isotopes have extremely short half lives and are no longer present today. However, recent studies looking at the chronological indicator Hf/W in iron meteorites have determined that differentiation of these bodies occurred much earlier than previously thought, within $\sim 10\text{m.y}$ of Solar System formation (Kleine et al., 2002; Wadhwa et al., 2006). This makes differentiated meteorites older than some of the undifferentiated, primitive meteorites, compelling us to reevaluate our current understanding of how and when differentiated and undifferentiated materials formed in the early Solar System. Current thoughts on the formation of primitive and undifferentiated asteroids are that the primitive asteroids formed continuously in early Solar System history. The asteroids that formed first, within the first 10m.y, differentiated because they contained more ^{26}Al .

The Dawn Mission

In September of 2007, NASA launched the Dawn mission, which will orbit and analyze the two largest asteroids in the main belt, Ceres and Vesta (Figs. 1 and 2)

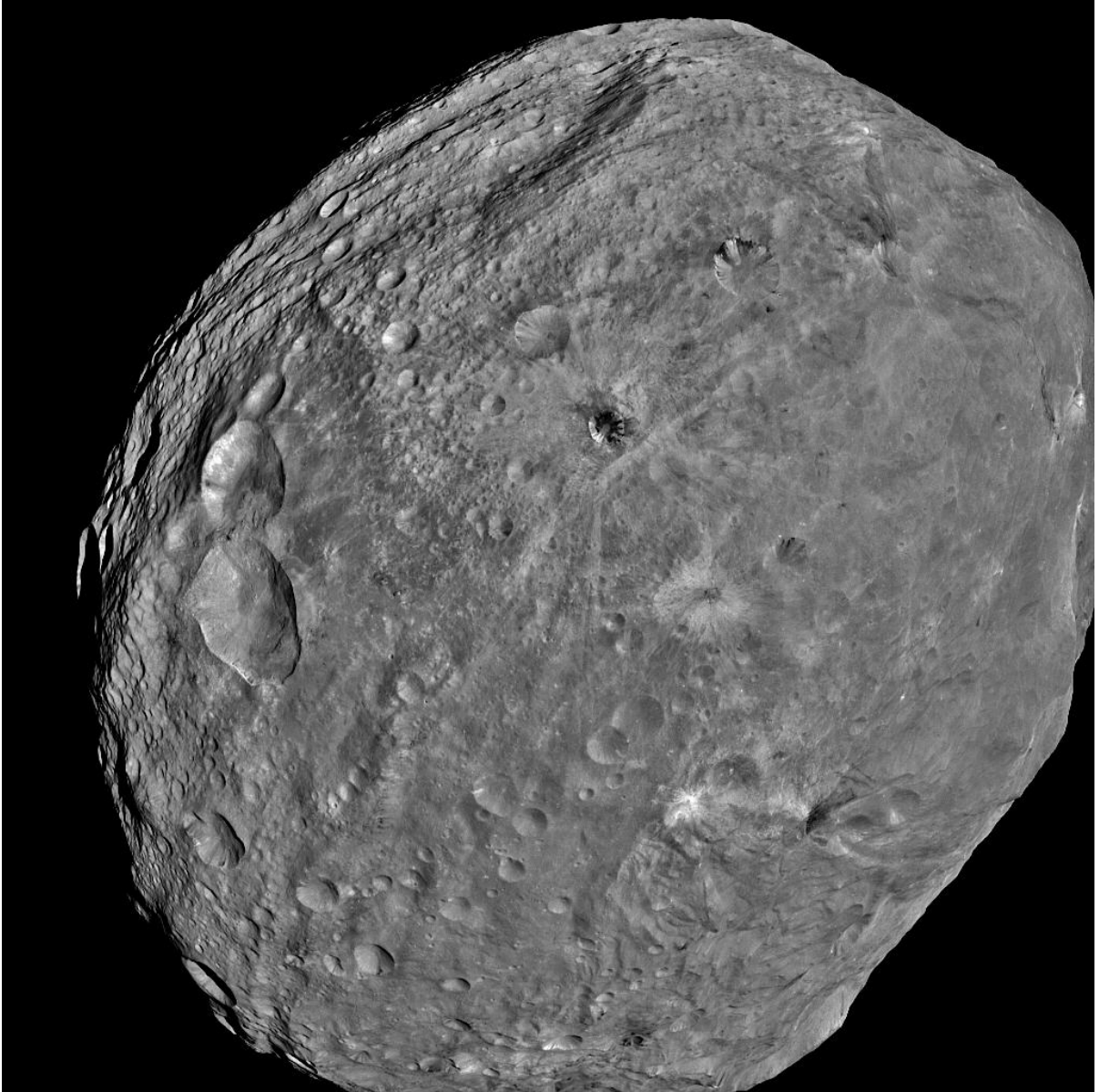


*Figure 1. Photo of Vesta by the Dawn spacecraft. (NASA/JPL-Caltech/
UCLA/MPS/DLR/IDA, 2011)*

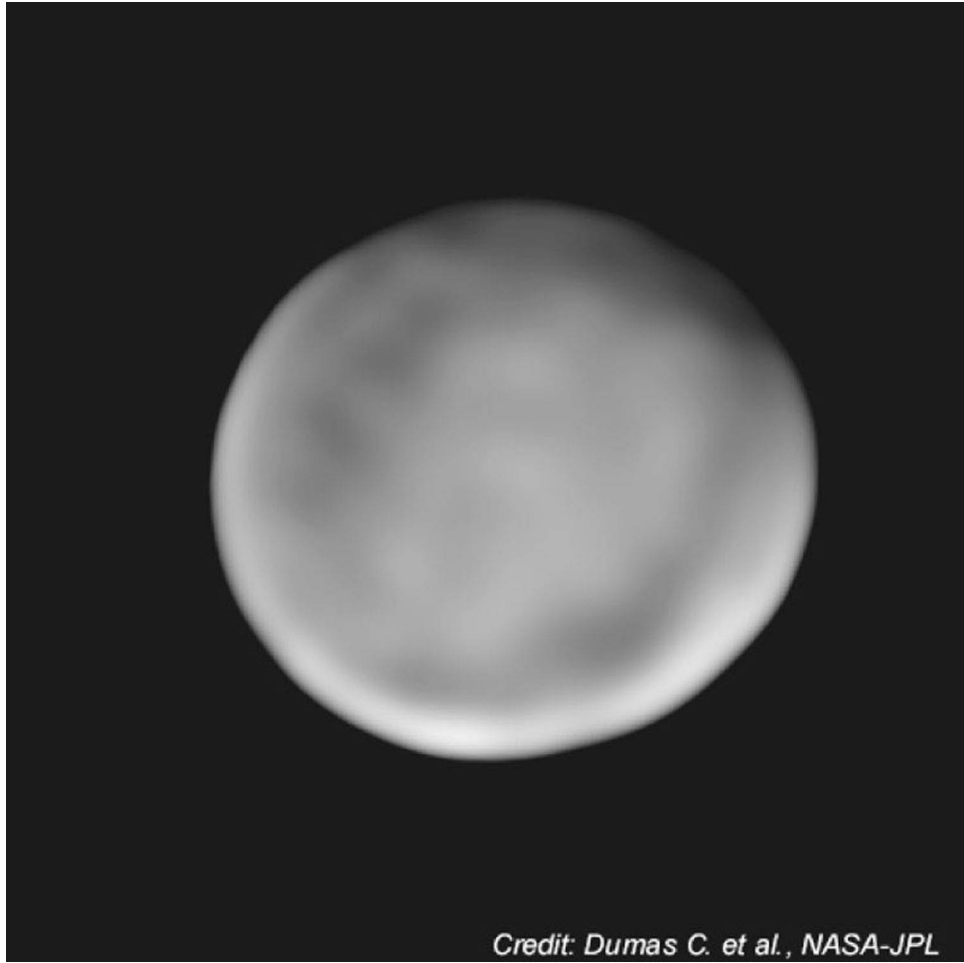


Figure 2. Ceres (C. Dumas, Keck Observatory (NASA-JPL), 2011)

Dawn's main objectives are to determine the roles of planetesimal size and the presence of water in the early formation of our Solar System (Russell et al., 2002; 2004). These objectives are especially important for understanding the formation of the terrestrial planets: Mercury, Venus, Earth, and Mars.

Ceres is a dwarf planet that was discovered in 1801 by Giuseppe Piazzi (Piazzi, 1801) and is the largest object in the asteroid belt between Mars and Jupiter. It is believed to be water-rich and likely formed in a similar environment to the outer planetary bodies, such as Jupiter's moon Ganymede (Russell et al., 2006). Some differentiation may have occurred, as density readings show that Ceres has a core and less dense material near the surface, thought to be water ice (Russell et al., 2004). Spectral evidence also suggests that the surface of Ceres contains abundant water-bearing minerals, lending more weight to the theory that it is a 'wet' body (NASA, 2007). The composition of these surface minerals is thought to be somewhat similar to that of primitive chondritic, unmelted meteorites (Russell et al., 2004).

Unlike Ceres, Vesta is a dry planetesimal with evidence of basaltic lava on its surface (Russell et al., 2004; 2006). It was discovered in 1807 by Wilhelm Olbers (Serio et al., 2002) and is the largest differentiated asteroid (~530km in diameter) (Thomas et al., 1997, Rayman et al., 2006). This makes it an ideal proxy for the formation of the terrestrial planets, because they are also differentiated. We can infer the origins and early formation of the terrestrial planets as well as get a better understanding of differentiation by studying Vesta and similar asteroids.

HEDs

As noted before, Vesta is the only object for which there is a known associated meteorite group. These samples, called the howardite-eucrite-diogenite (HED) suite, consist of volcanic (basaltic eucrites), plutonic (cumulate eucrites and diogenites), and brecciated (howardite) rocks derived from the same basaltic magma (Figs. 3a-c) (McSween, 1999). HEDs account for approximately 5% of all meteorites that land on Earth (Meteoritical Bulletin Database) and are the most abundant group of differentiated, achondritic meteorites. Eucrites represent the crust of Vesta, similar to basalts and gabbros on Earth, and they range in texture from glassy, quenched samples to coarser grained rocks that have been recrystallized by metamorphism. The difference between terrestrial and eucritic basalts is that eucrites contain Ca-rich plagioclase with little Na, as well as low-Ca pyroxene pigeonite, and have no trace of hydrated minerals (McSween, 1999). Diogenites are cumulate orthopyroxenites that cooled slowly at depth and are plutonic, coarse-grained meteorites. They are somewhat similar in composition to eucrites but have smaller modal abundances of plagioclase and contain abundant Mg-rich orthopyroxene, enstatite (McSween, 1999). Howardites are brecciated meteorites containing both eucritic and diogenitic material. They provide definitive evidence that eucrites and diogenites come from the same parent body, as well as showing evidence for impacts on that parent body. In order for howardites to form, impacts would have had to excavate into the deeper, plutonic (diogenite) material on the asteroid, allowing them to incorporate both diogenetic and eucritic material.

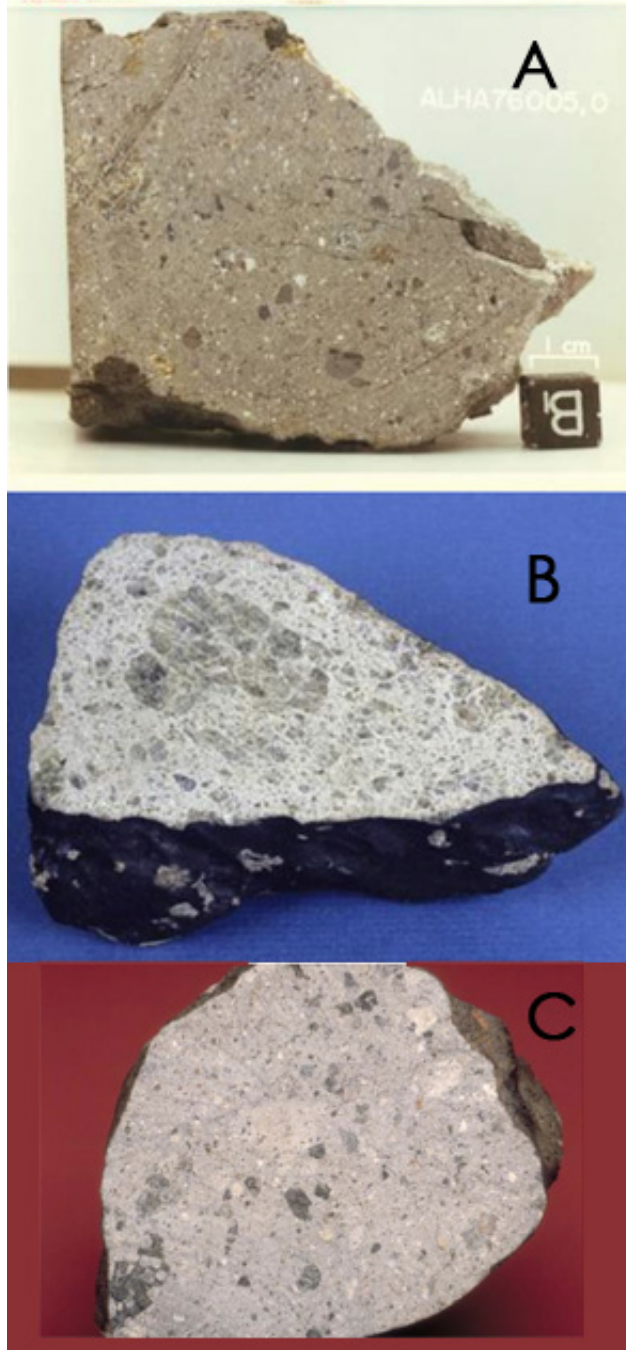


Figure 3: (A) A polymict eucrite (1cm cube in photo for scale), (B) diogenite (sample is 7cm wide), (C) howardite (sample is 5cm wide) (Richter and Garber, 2011)

Oxygen isotopes also tie the formation of the HEDs to a single parent body. Oxygen isotope signatures can be traced back to interactions between the solar nebula and materials in parent bodies, and also preserve evidence of any subsequent changes in the parent body (Clayton and Mayeda, 1996). Clayton and Mayeda (1996) showed that the HED oxygen isotope signatures are indeed consistent with this group of meteorites coming from a single parent body.

While the oxygen isotopes and the brecciated nature of howardites tell us that the HEDs come from the same parent body, they do not link them directly to Vesta. McCord et al., (1970) were the first to note the similarity between the visible and infrared reflectance spectra from the HEDs and Vesta (Fig. 4). The similar spectra suggest that Vesta is the parent body of the HEDs (McCord et al., 1970; Clayton and Mayeda, 1996; Drake, 2001). However, the Vesta-HED link was not initially accepted, due to Vesta's position in the main belt. It is dynamically unlikely for fragments from Vesta (the HEDs) to be transported to Earth (Wasson and Wetherill, 1979). Any impacts that would break pieces off of Vesta would also have to have implausible velocities for fragments to make it to Earth (Keil, 2002).

Vestoids

Using visible and near-infrared reflectance spectra, Binzel and Xu (1993) discovered basaltic main belt asteroids (<10km in diameter) that are dynamically linked to Vesta. These asteroids, known as Vestoids, have given us insight into how we receive HED meteorites on Earth (Binzel and Xu, 1993). The Vesta-like asteroids are

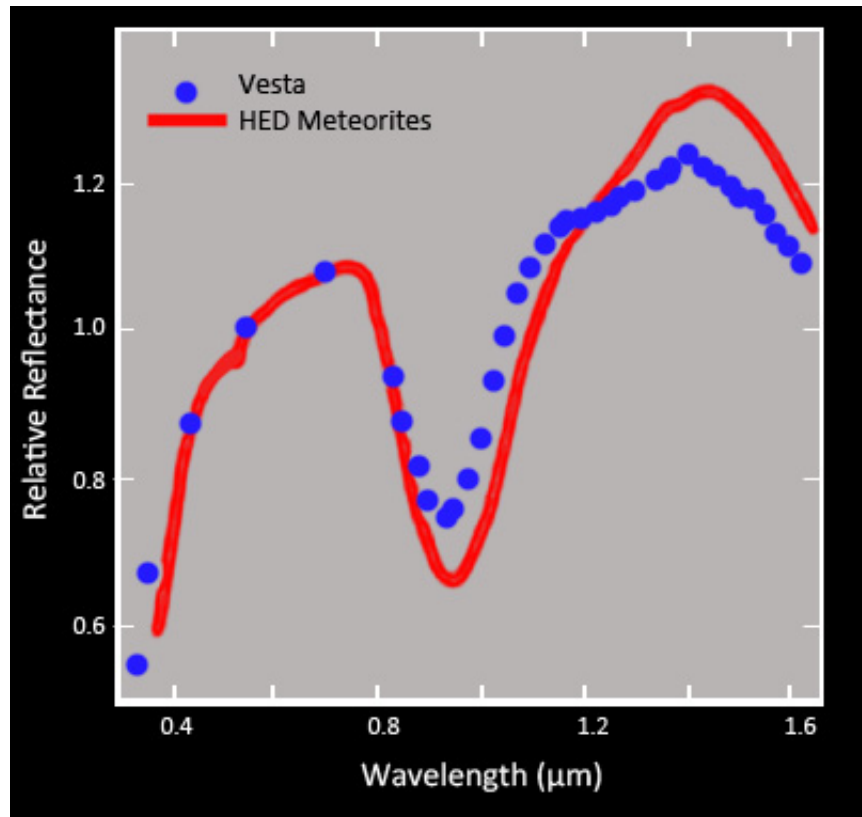


Figure 4: Spectral data comparing Vesta and the HEDs. Similar curves suggest that Vesta is indeed the parent body of the HEDs (Adapted from McCord et al., 1970).

collisional fragments that are a result of one or multiple impacts on Vesta, as evident in the large crater on Vesta's South Pole (Thomas et al., 1997). Jupiter's gravitational influence can perturb an object's orbit, in this case the Vestoids, so that it becomes increasingly elliptical. This can alter an orbit to such an extent that it becomes Earth-crossing, causing the object to collide with Earth. These areas of gravitational influence are called resonances or Kirkwood gaps (Fig 5). The Vestoids lie between Vesta and the 3:1 orbit-orbit resonance (2.5 AU) with Jupiter (Fig. 6), a known delivery path for meteorites to Earth. Figure 6 shows Vesta and the Vestoids relative to the 3:1 Kirkwood Gap. Vesta is quite a distance from the 3:1 resonance, while the Vestoids are widespread within the main belt and reach right up to the 3:1 resonance. This makes the Vestoids the likely source of HED meteorites (Drake, 2001).

Competing Models of Formation for Vesta

Any model proposed must be able to explain the varying geochemical compositions seen in the HEDs. The eucrites can be classified into basaltic and cumulate-type members. The basaltic eucrites can be further divided in terms of their geochemistry into the Main Group-Nuevo Laredo and Stannern trends (Fig. 7). The Main Group-Nuevo Laredo trend is defined by increasing incompatible elements with decreasing Mg number ($Mg/Mg+Fe$) and makes up the most abundant eucrite trend (Stolper, 1977; Mittlefehldt and Lindstrom, 2003). The Stannern trend also shows increasing abundances of incompatible elements but with only a slight decrease in Mg number (Stolper, 1977; Mittlefehldt and Lindstrom, 2003) (Fig. 7). Vesta's formation is

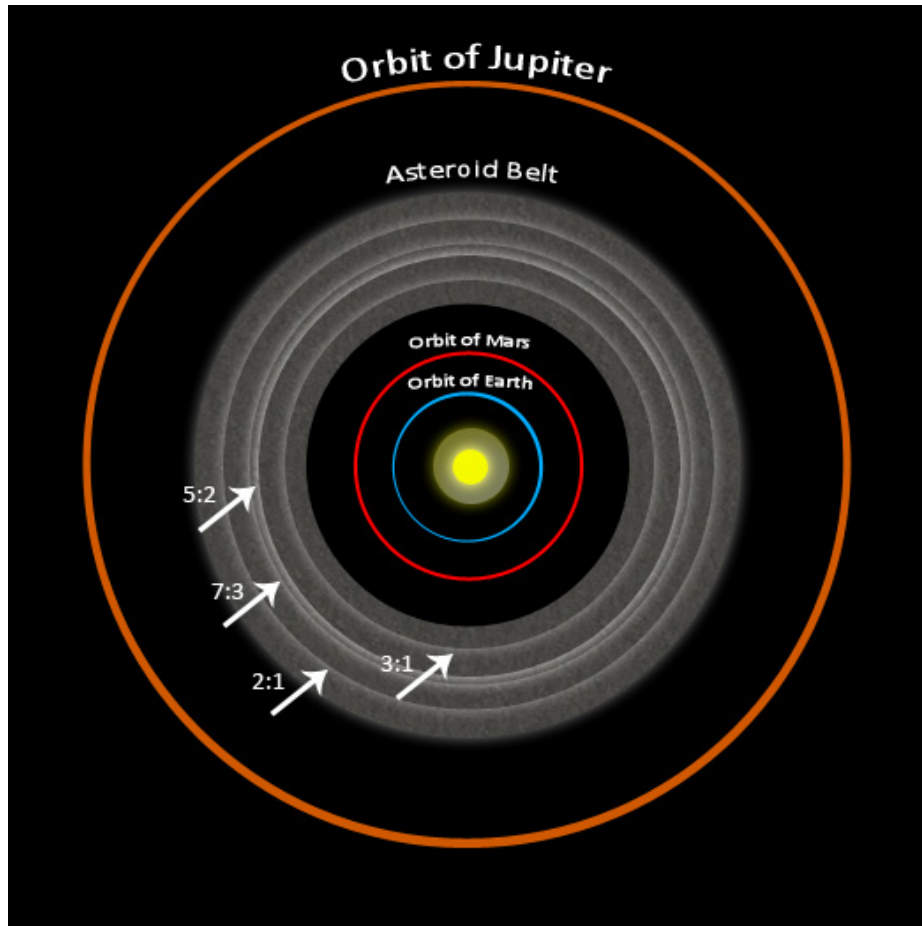


Figure 5: Location of Kirkwood gaps, such as the 3:1 gap, in the main belt between Mars and Jupiter (Adapted from Miller, 2008).

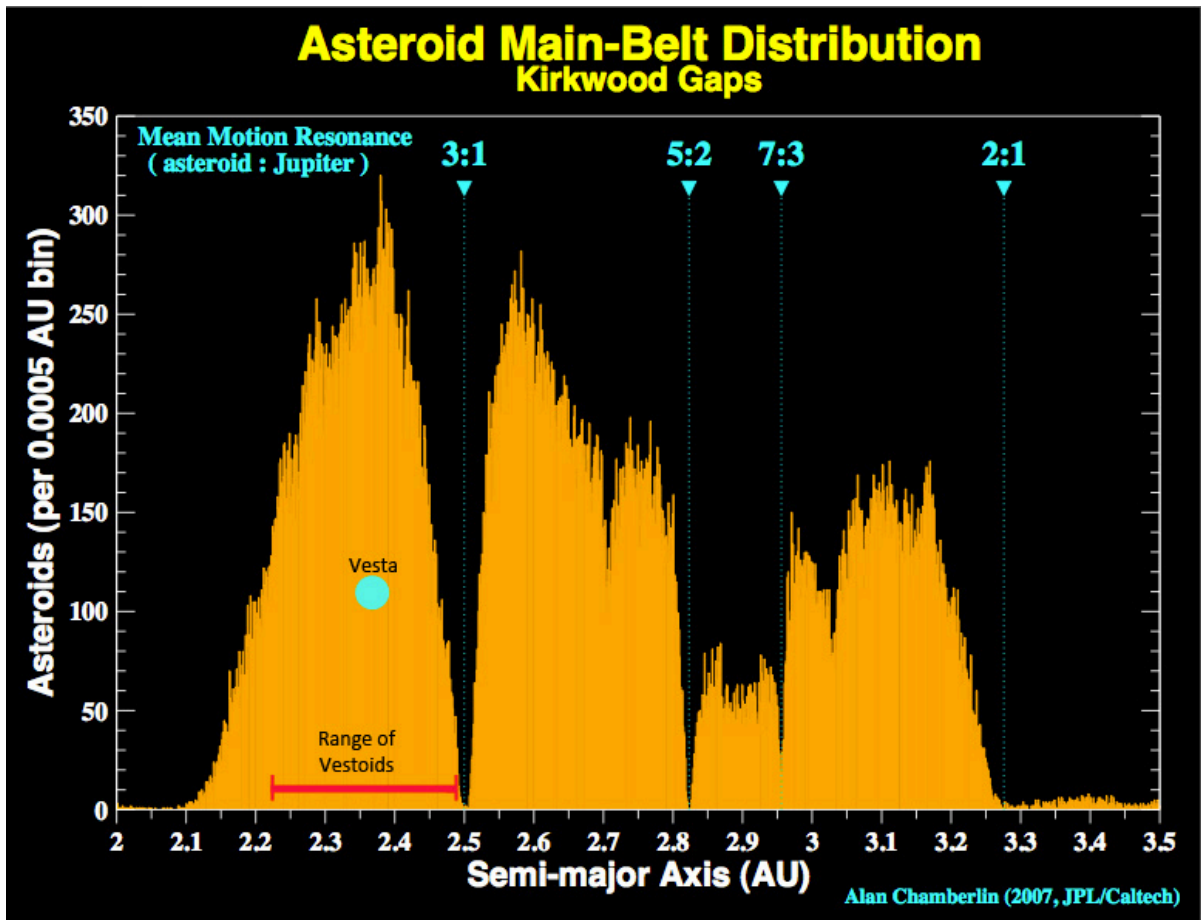


Figure 6: The 3:1 Kirkwood gap (2.5 AU) showing the position of Vesta and the Vestoids in the main belt relative to the rest of the asteroids around them (Adapted from Chamberlin, 2007).

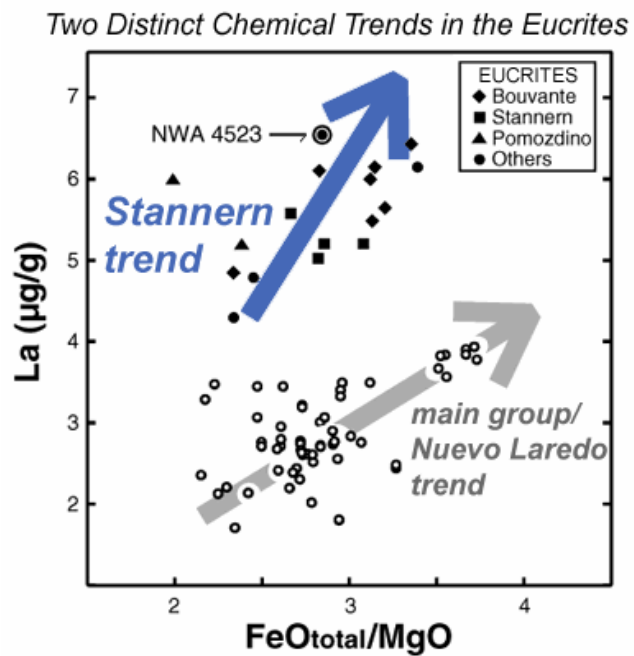


Figure 7: The Stannern and Main Group-Nuevo Laredo trends (Adapted from Taylor, 2009).

not well understood and several models have been suggested to explain it, which are discussed further below.

Models of Formation: Fractional Crystallization

Mason (1962) proposed a fractional crystallization model to account for the differences in eucrite composition. The problem with this model is that while the Main Group-Nuevo Laredo trend can be explained by the fractional crystallization of pigeonite and plagioclase, the Stannern trend cannot. Thus, this model is incapable of producing the relationship between the Main Group-Nuevo Laredo and Stannern trend.

Models of Formation: Partial Melting

The partial melting model involves a single source region with primary magmas produced by different degrees of partial melting (Stolper, 1977). However, the siderophile element concentrations of the Nuevo Laredo and Stannern trends cannot be produced using the partial melting model. Siderophile element contents have been used to argue that metal was separated from silicate before the eucrite parent melts formed (Mittlefehldt and Lindstrom, 2003), and this separation could only occur when the parent body contained a large fraction of melt. The partial melting model would predict the siderophile element tungsten (W) to be constant throughout the eucrites because of buffering by metal in the source region (Mittlefehldt and Lindstrom, 2003). However, we know that W is highly variable between eucrites (Mittlefehldt and Lindstrom, 2003). This means that different source regions would need to have different metal contents.

Models of Formation: Magma Ocean

A popular theory is that a magma ocean developed after Vesta had accreted (Righter and Drake, 1997; Ruzicka et al., 1997). The model of Righter and Drake (1997) maintains that while Vesta was still in a molten state, convection kept the magma stirred up and equilibrium crystallization began. After convection started to cease, the crystals and melt started to segregate, leaving behind residual magmas. These residual magmas eventually formed the Main Group and Stannern trend eucrites. The Main Group went through fractional crystallization and formed the Nuevo Laredo trends. Diogenites formed prior to fractional crystallization. The problem with this model is that the orthopyroxene within the diogenites show large chemical variations, whereas the magma ocean model predicts their composition should be relatively constant. The chemical variations are thought to be caused by multiple mafic parent melts and suggest efficient fractional crystallization occurred before the formation of residual melts (Mittlefehldt and Lindstrom, 2003). Thus, the geochemistry of the diogenites is not consistent with equilibrium crystallization of a molten body (Mittlefehldt and Lindstrom, 2003; Righter and Drake, 1997).

While no one theory has yet successfully explained the differences in geochemistry between the HEDs, the magma ocean and partial melting model are currently the most accepted ways to explain the petrogenesis of Vesta.

Testing Models for the Formation for Vesta

Recent work by Mayne et al. (2010) suggests that unequilibrated eucrite samples could be key in distinguishing between the partial melting model and magma ocean

model. Before I discuss why unequilibrated eucrites are so important to understanding the formation of Vesta, I will first define how equilibration is determined in eucrites.

Thermal Metamorphism in Eucrites

Most eucrites have undergone some type of subsolidus reheating event, suggesting that a global thermal metamorphic event occurred on Vesta during or after crustal formation. It is commonly thought that this global thermal metamorphism is a result of the eruption, rapid cooling, and subsequent burial and reheating of successive lava flows on the surface of Vesta (Yamaguchi et al., 1996). Traditionally, the pyroxene quadrilateral compositions (hereafter referred to as ‘major element compositions’ after Mayne et al., 2010) have been the main tool for assessing if a eucrite is equilibrated, i.e. if it has been thermally metamorphosed (Pun and Papike, 1996). The pyroxenes in eucrites show three different major element trends (Fig. 8). The Mg-Fe-Ca trend (Fig. 8a) and Mg-Fe trend (Fig. 8b) are found in eucrite pyroxenes that retain their original zonation, and are therefore unequilibrated. The Fe-Ca trend (Fig. 8c) is observed in a eucrite where the pyroxene has exsolved high-Ca augite lamellae from low-Ca pigeonite. The Fe-Ca trend, therefore, shows equilibration of the major elements. For example, both ALH A81001 and Serra de Magé (Figs. 8d,e) show equilibrated major element pyroxene trends.

Mayne et al. (2010) noted that the minor elements in pyroxene (Cr, Al, Ti) in many “equilibrated” eucrites show large compositional variations. This indicates that the pyroxene is only partially equilibrated and some of the original compositional zonation still remains. This means that some information about the crystallization history of the eucrite can still be gleaned from its pyroxene composition. Cr is a

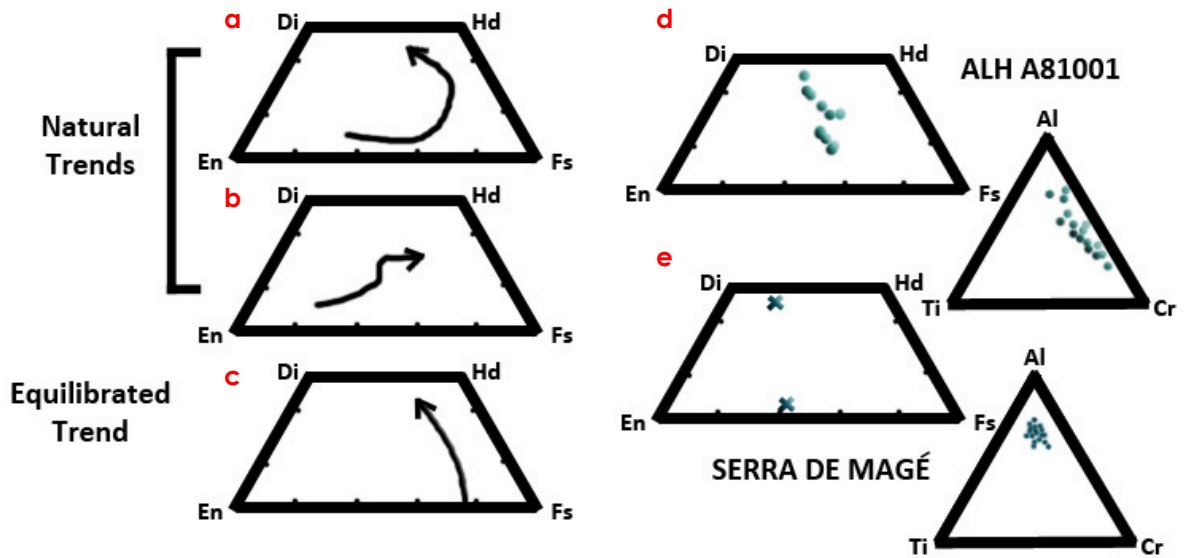


Figure 8: Pyroxene equilibration trends for the major elements (En, Fs, Wo). Trends (a) and (b) are natural, unequilibrated trends, while (c) illustrates an equilibrated trend. The diagrams to the right show equilibrated major elements in pyroxene next to ternary diagrams of minor elements (Adapted from Mayne et al., 2009)

compatible element with pyroxene; therefore, the earliest crystallized pyroxenes are rich in Cr. As crystallization continues, the melt becomes more Al-rich, as do the pyroxenes, until plagioclase starts to crystallize, essentially 'using up' the Al. This drives the melt and the pyroxenes towards more Ti-rich compositions (Fig. 9). This trend from Cr to Al to Ti-rich can be used to tell us how evolved the melt was when the rock was crystallizing. The more Cr-rich the pyroxenes are, the more primitive the melt, while the Ti-rich trends crystallize from more evolved melts. Plagioclase grains in some eucrites also show significant zoning and have a large range of anorthite content. Equilibration in plagioclase depends on the range of anorthite content. An anorthite range of <5mol% is considered an equilibrated plagioclase, and a range larger than 5mol% would be unequilibrated and plagioclase zoning would likely be present.

This discrepancy in so-called "equilibrated" eucrites caused Mayne et al. (2010) to reevaluate how an equilibrated eucrite is classified. They identified three components, major and minor elements in pyroxene and range of anorthite content in plagioclase, to be used to quantitatively assess equilibration of eucrites. These three components equilibrate at different temperatures due to the different diffusion rates for elements within minerals. Plagioclase is more resistant to thermal metamorphism than pyroxene, due to the slow Si-Al diffusion kinetics in the coupled albite-anorthite substitution compared to the kinetics of Fe-Mg diffusion in pyroxene (O'Neill and Delaney 1982; Mayne et al., 2010).

I will use the Mayne et al. (2010) criteria outlined above when determining equilibration for eucrite samples in this study.

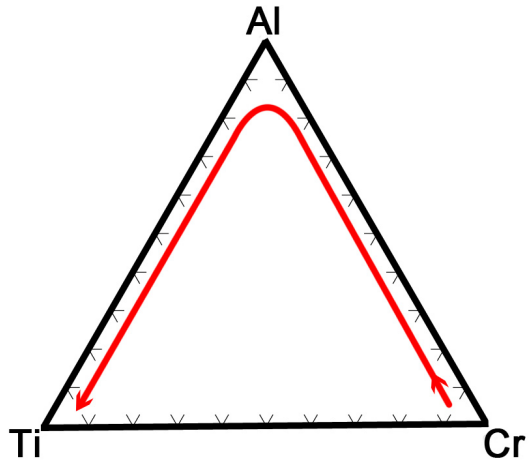


Figure 9: Minor element trends of pyroxene (Cr, Al, Ti). The pyroxenes start off Cr-rich, and trend towards the Al-rich end member until plagioclase starts to form, and at which time the pyroxenes trend to the Ti-rich end.

Testing Models for Formation of Vesta: Using ALH A81001

ALH A81001 is a quench-textured eucrite, which must have cooled quickly after its formation (Fig 10). Unlike most eucrites, ALH A81001 has not been fully re-equilibrated by thermal metamorphism (Mayne et al., 2010). It has an equilibrated major element trend, but minor element data show that it is not a fully equilibrated eucrite. As a result, the mineral phases within it retain much of their original chemical zonation. ALH A81001 contains Cr-rich pyroxene, which suggests it came from a primitive melt (Fig. 8d). Mayne et al. (2010) realized that the unique crystallization history, evolution, and thermal history of ALH A81001 make it an ideal sample to test the two competing models for Vesta's formation, because it would form in two very different environments depending on which model is correct.

When considering the formation of ALH A81001 in the partial melting model, there are several factors to keep in mind. Firstly, ALH A81001 must have formed at or near the surface of Vesta, because it underwent rapid cooling. It must have crystallized late in Vesta's formation because it has not been fully equilibrated, yet it must also be from a primitive melt as it contains Cr-rich pyroxenes. Therefore, ALH A81001 must have formed from a late-stage primitive melt on or near the surface of Vesta (Fig. 11). If it formed in an intrusive body beneath the surface, it must have formed at a quench margin. This would result in small, localized melts, and eucrites like ALH A81001 would be rare and not abundant on the surface.

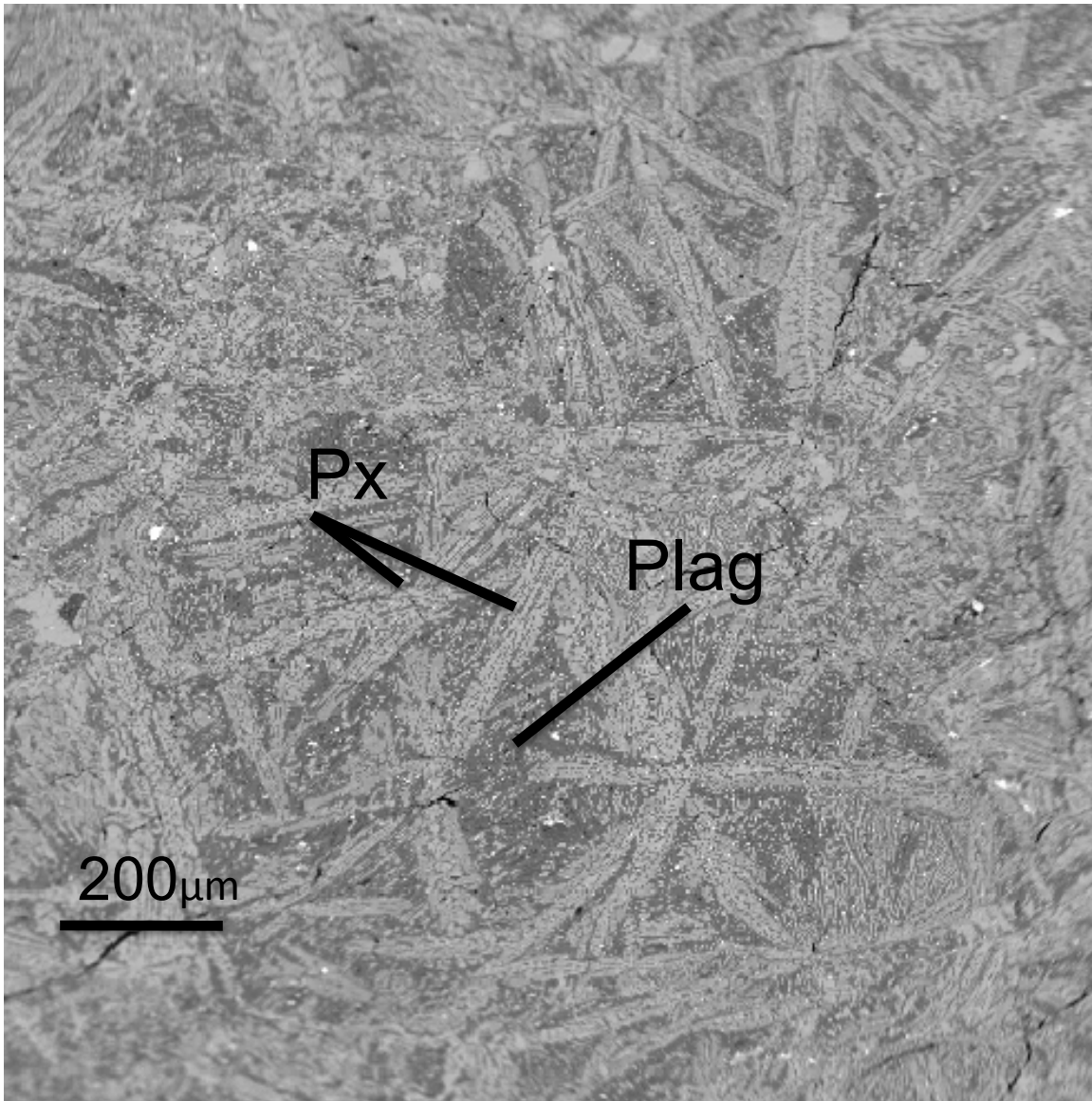


Figure 10: BSE image of ALH A81001 showing skeletal pyroxene and plagioclase grains. The small scale of the BSE image denotes how fine grained the sample is (adapted from Mayne et al., 2009).

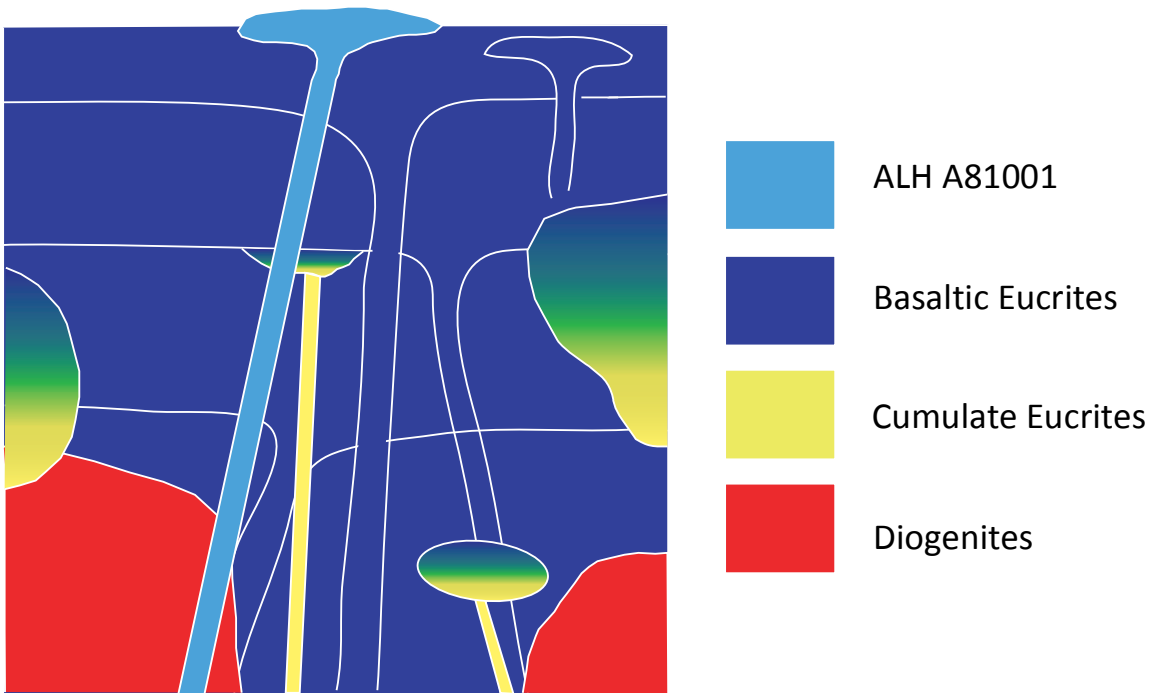


Figure 11: Partial melting model illustrating the formation of ALH A81001.

In the magma ocean model, the formation of ALH A81001 is harder to explain. Cr-rich pyroxenes would crystallize early and would sink in the magma ocean, forming part of the cumulate pile. These pyroxenes would be equilibrated and this environment would not result in a quench-textured eucrite, such as ALH A81001. The only location ALH A81001 could have formed in a magma ocean setting is as a quench crust (Fig. 12). The magma ocean would lose significant heat to space and, therefore, would form an early (Cr-rich) fast-cooled crust, which would insulate the magma beneath it. Since the quench crust would have been of global event, we would expect to see units like ALH A81001 widespread across Vesta, as well as expect them to be abundant in the eucrite collection.

A summary of the ALH A81001 formation predictions for these two competing models is shown in Table 1.

Individual fine-grained eucrites, like ALH A81001, are not common (Mayne et al., 2010; Russell et al., 2004; Stolper, 1977). However howardites, the most abundant member of the HED family, can contain unique, fine-grained eucrite clasts of a type not found in meteorites consisting only of eucrites (from here on, when I refer to eucrites, I'm referring to eucrite clasts). In this study, we looked at the entire howardite collection at the National Meteorite Collection at the Smithsonian Institution National Museum of Natural History to find additional fine-grained eucrite clasts. Studies by Mayne et al. (2009) indicate that fine-grained eucrites may be less equilibrated and, therefore, may retain their original pyroxene zonation. Their abundance may help us differentiate between the two competing models of Vesta's formation (Table 1).

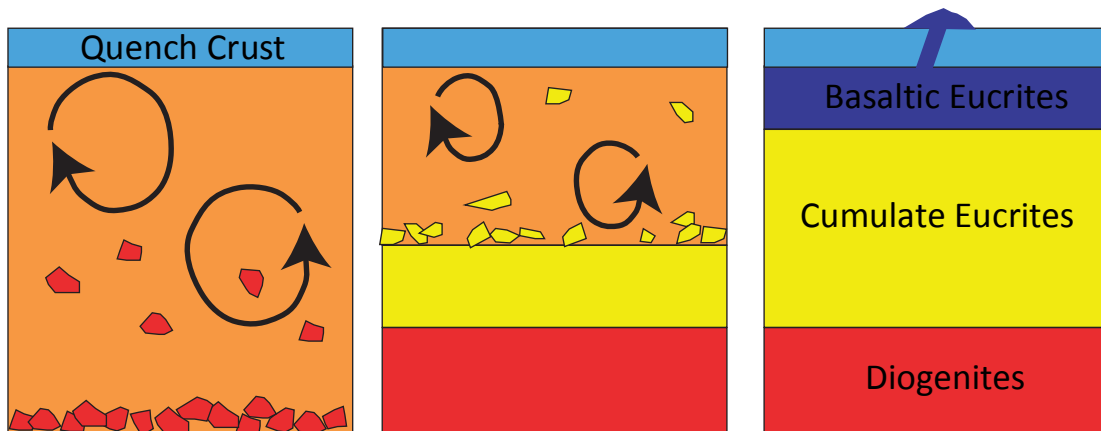


Figure 12. Magma ocean model illustrating the quench crust and formation of the diogenites, cumulate eucrites, and basaltic eucrites. In this model ALH A81001 could have formed in the quench crust.

Table 1: Comparison of the formation environment for ALH A81001 in the partial melting and magma ocean models.

Partial Melting	Magma Ocean
From a late stage partial melt	Formed earlier from quench crust
Small-scale distribution - Localized event	Large-scale distribution - Global event

Furthermore, fine-grained eucrites in howardites are valuable to study as they have not been comprehensively examined previously and may enable us to increase our knowledge of the crustal processes during differentiation and terrestrial planetary formation.

Methodology

Samples

In this study, all howardite thin sections (1in. rounds or 2.5cm) in the Antarctic and non-Antarctic National Meteorite Collection at the Smithsonian Institution's National Museum of Natural History were examined for the presence of fine-grained eucrite clasts (Table 2). The reason we did not use of the Oscar E. Monnig Meteorite collection is that it does not contain many HED samples that are already thin sectioned. The National Meteorite Collection at the Smithsonian not only has the largest collection of howardites, but thin sections of these howardites have already been made. Some howardites had multiple sections and in these cases every section was examined. Eight fine-grained eucrite clasts were identified in five howardites (Table 3).

SEM Maps

All clasts were analyzed using the FEI NovaSEM 600 scanning electron microscope in the Mineral Sciences Department at the Smithsonian, operating at 15kV. Elemental X-ray maps and back-scattered electron (BSE) images were produced and examined to determine minerals present, modal abundances, and textures. The magnification used for each individual clast (Table 3) was dependent on clast size, texture of the clast, appropriate resolution and time allotted to collect data. The manner in which the SEM maps each sample is through a quadrant system (Fig. 13a). The SEM starts at the top left-hand corner with (0,0) and continues across the top (1,0), (2,0) (3,0), etc., until it starts back at the left-hand side starting on the second row (Fig. 13b).

Table 2: All howardites examined in this study.

Allan Hills 09004	Jodzie	Northwest Africa 1653	Northwest Africa 5957	Yamato 793497
Allan Hills 88102	Kapoeta	Northwest Africa 1664	Northwest Africa 5959	Yamato 793541
Allan Hills 88135	LaPaz Icefield 04838	Northwest Africa 1695	Northwest Africa 6073	Yamato 793543
Allan Hills A78006	Larkman Nunatak 06621	Northwest Africa 1769	Northwest Africa 6178	Yamato 793544
Asuka 881170	Las Colonas	Northwest Africa 1819	Northwest Africa 6206	Yamato 793546
Bholghati	Le Teilleul	Northwest Africa 1914	Old Homestead 001	Yamato 793550
Bununu	Lewis Cliff 85313	Northwest Africa 1929	Pavlovka	Yamato 793577
Camel Donga 004	Lewis Cliff 85441	Northwest Africa 1939	Pecora Escarpment 02009	Yamato 82049
Chaves	Lewis Cliff 87005	Northwest Africa 1942	Pecora Escarpment 02013	Yamato 82091
Dar al Gani 669	Lewis Cliff 87015	Northwest Africa 1943	Pecora Escarpment 02014	Yamato 86795
Dar al Gani 671	Lewis Cliff 87053	Northwest Africa 2060	Pecora Escarpment 02015	Yamato 981604
Dar al Gani 779	Lohawat	Northwest Africa 2132	Pecora Escarpment 02016	Yurtuk
Dar al Gani 881	Luotolax	Northwest Africa 2226	Pecora Escarpment 02018	Zmenj
Dar al Gani 915	MacAlpine Hills 02666	Northwest Africa 2251	Pecora Escarpment 02019	
Dar al Gani 932	MacAlpine Hills 02703	Northwest Africa 2379	Pecora Escarpment 02065	
Dhofar 018	MacAlpine Hills 041269	Northwest Africa 2480	Pecora Escarpment 02066	
Dhofar 1302	Mässing	Northwest Africa 2641	Queen Alexandra Range 93008	
Dhofar 455	Melrose (b)	Northwest Africa 2644	Queen Alexandra Range 93723	
Dhofar 485	Meteorite Hills 96500	Northwest Africa 2698	Queen Alexandra Range 94200	
Elephant Moraine 83376	Meteorite Hills 00423	Northwest Africa 2738	Queen Alexandra Range 94616	
Elephant Moraine 87503	Meteorite Hills 00427	Northwest Africa 2739	Queen Alexandra Range 97001	
Elephant Moraine 87512	Meteorite Hills 00800	Northwest Africa 2752	Queen Alexandra Range 97002	
Elephant Moraine 87513	Meteorite Hills 01082	Northwest Africa 2794	Queen Alexandra Range 99033	
Elephant Moraine 87528	Meteorite Hills 01087	Northwest Africa 2819	Queen Alexandra Range 99058	
Elephant Moraine 92014	Miller Range 05062	Northwest Africa 2853	Sahara 99076	
Elephant Moraine 92015	Miller Range 05085	Northwest Africa 2873	Sahara 99314	
Elephant Moraine 92022	Miller Range 05165	Northwest Africa 2890	Sandford Cliffs 03472	
Elephant Moraine 96002	Miller Range 07007	Northwest Africa 3117	Scott Glacier 06040	
Elephant Moraine 96003	Miller Range 07009	Northwest Africa 3149	Washougal	
Elephant Moraine 96004	Miller Range 07661	Northwest Africa 3311	Winterhaven	
Elephant Moraine 99400	Miller Range 07663	Northwest Africa 4289	Yamato 7308	
Elephant Moraine 99408	Miller Range 07664	Northwest Africa 4585	Yamato 790727	
Elephant Moraine 99443	Miller Range 07665	Northwest Africa 4826	Yamato 790991	
Erevan	Miller Range 090153	Northwest Africa 4858	Yamato 791064	
Frankfort (stone)	Molteno	Northwest Africa 4869	Yamato 791074	
Geologists Range 99120	Monticello	Northwest Africa 4934	Yamato 791192	
Graves Nunataks 98030	Mount Crean 01400	Northwest Africa 5199	Yamato 791206	
Graves Nunataks 98168	Mount Pratt 04401	Northwest Africa 5208	Yamato 791207	
Grosvenor Mountains 95534	Mount Pratt 04402	Northwest Africa 5222	Yamato 791208	
Grosvenor Mountains 95535	Muckera 001	Northwest Africa 5306	Yamato 791424	
Grosvenor Mountains 95574	Muckera 002	Northwest Africa 5350	Yamato 791448	
Grosvenor Mountains 95581	Mundrabilla 018	Northwest Africa 5415	Yamato 791489	
Grosvenor Mountains 95602	Mundrabilla 020	Northwest Africa 5485	Yamato 791492	
Grosvenor Mountains 95633	Northwest Africa 776	Northwest Africa 5487	Yamato 791497	
Hammadah al Hamra 285	Northwest Africa 1150	Northwest Africa 5489	Yamato 791573	
Hughes 004	Northwest Africa 1181	Northwest Africa 5614	Yamato 793173	
Hughes 005	Northwest Africa 1182	Northwest Africa 5724	Yamato 793192	
Jiddat al Harasis 556	Northwest Africa 1282	Northwest Africa 5743	Yamato 793252	

Table 3: Magnification used to analyze SEM mineral maps. Colors indicate individual howardite samples.

Clasts	Magnification
MIL 07664,4A	206
MIL 07664,4B	208
QUE 99033,2A	210
QUE 99033,2B	300
QUE 97001	230
EET 96002	258
ALH A090004A	280
ALH A090004B	280

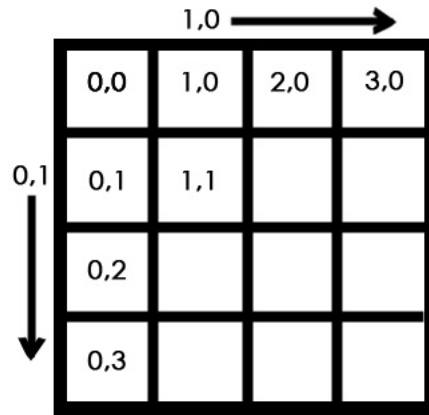


Figure 13a: The SEM maps data through a quadrant system.

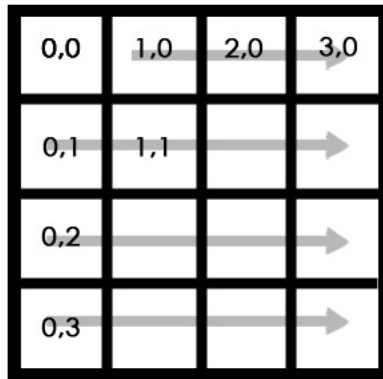


Figure 13b: The SEM starts to map at the top left-hand corner to the right edge of the map, making the first row. Then it starts back on the left-hand side to start the second row.

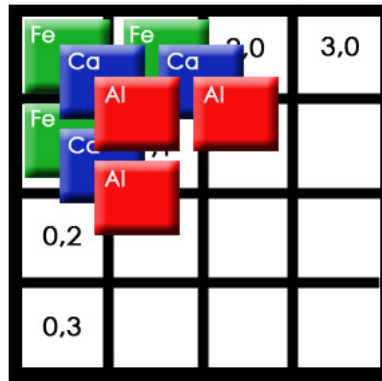


Figure 13c: Each tile consists of multiple elemental X-ray map layers in a particular order. Once all of the tiles are in place, we can separate individual element maps out by layer.

The number of tiles is defined by the resolution used, the area mapped and the tile overlap needed to completely map the clasts. Each tile consists of multiple layers, and each layer represents a different elemental X-ray map (Fig. 13c). For this study we collected data for Ca, Al, Fe, Si, Mg, O, C, Cr, K, Mn, Na, S, and Ti, as well as a BSE image. Each pixel of these maps represents a spectrum of compositional information.

After the SEM has produced all of the tiles necessary to complete the map, the stacks of element tiles are matched together according to their place on the quadrant grid. Once each stack is matched up correctly, each individual element map is merged together with all of its tiles (i.e. All Fe tiles). For example, all tiles of Fe on the quadrant grid would be merged together to form one Fe map. These element maps are then separated to view on an individual basis.

To form the mineral maps, we took the element maps of interest, Al, Fe and Ca, needed to identify plagioclase, and low-Ca and high-Ca pyroxene, respectively (Fig. 14) and made them slightly transparent. This allows for all of the element map colors to show through and blend together for us to easily identify minerals and opaque phases within the clast (Fig. 14). Opaque phases, such as sulfides, oxides, and iron, are identified by looking at individual and combined elemental X-ray maps. For example, combining Fe and S can identify sulfides. Ni was not sampled in this study, thus we cannot assess if there is FeNi in any samples.

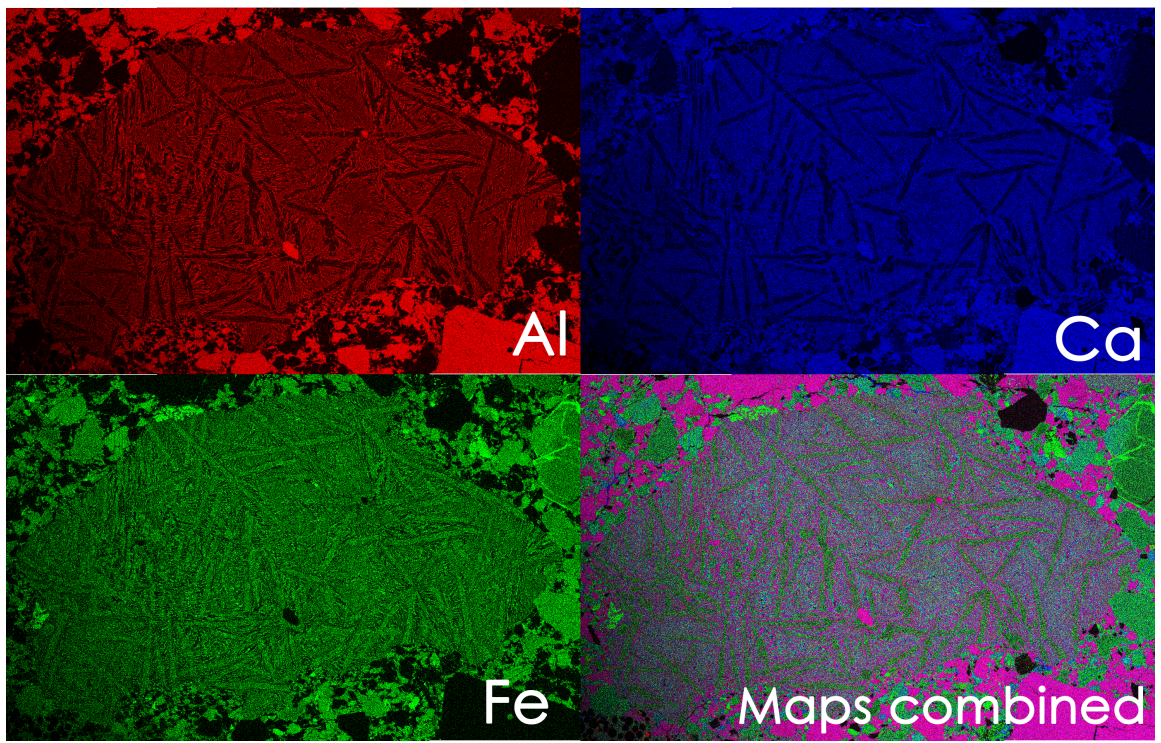


Figure 14: An example of SEM element maps used to represent minerals when combined.

Electron Microprobe

The compositions of pyroxene and plagioclase grains within each of the clasts were analyzed using the JEOL 9800R/5 electron microprobe, also at the Smithsonian. Analytical conditions for the electron microprobe were 20nA, 15kv, and 1-2 micron beam size. We tried to focus our microprobe sampling on different compositions and textures seen throughout the clasts (Fig. 15). Due to the fine-grained nature of these clasts, it was difficult to sample any zonation seen in the SEM data. The microprobe beam had to be centered on the grains to achieve a good analysis. Raw oxide and cation data were obtained and normalized to establish detailed mineral chemistry of the samples.

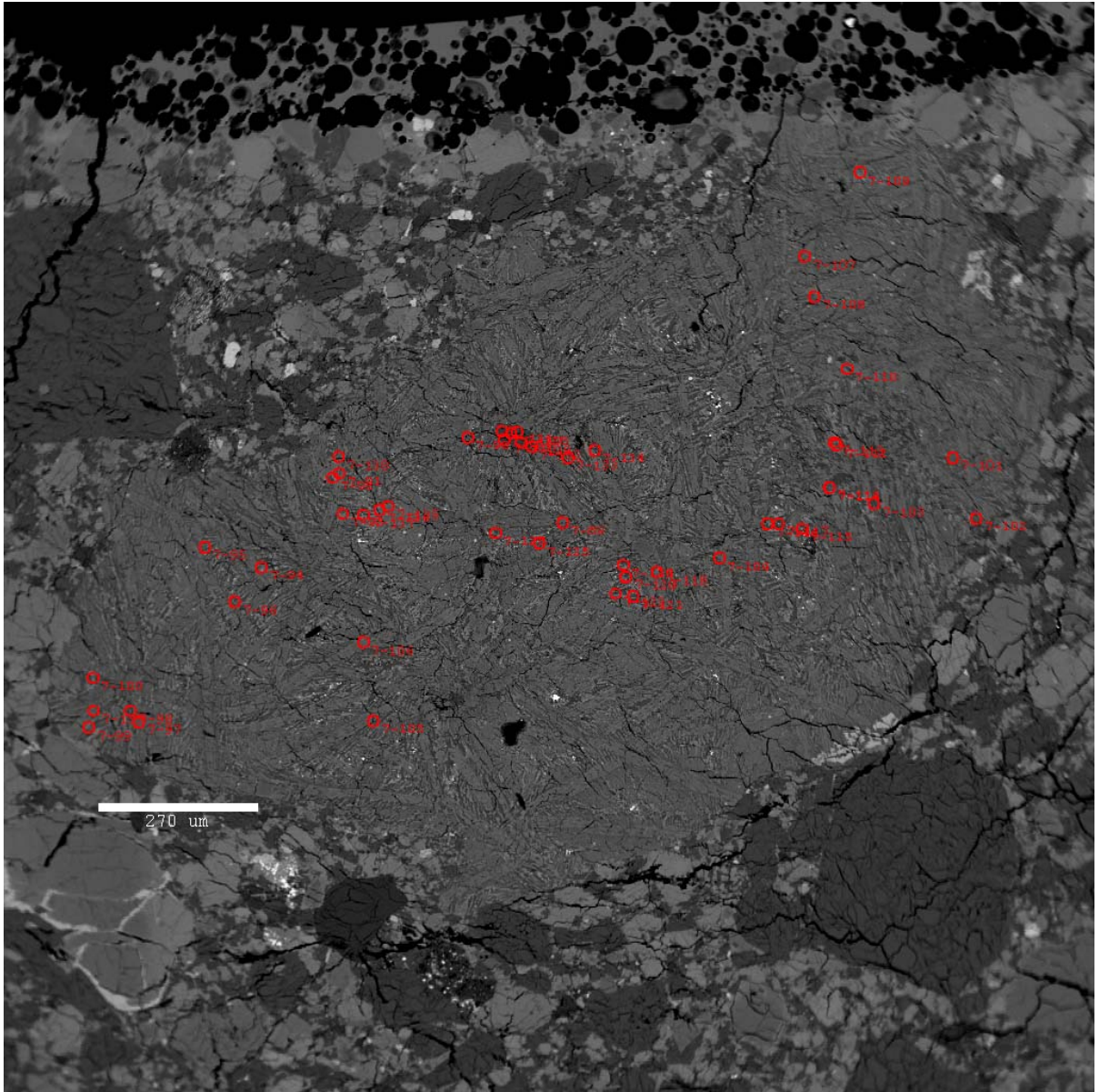


Figure 15. BSE image of MIL 07664,4B. Points analyzed by the electron microprobe.

Results

One of the main objectives of this study is to assess the degree of equilibration caused by thermal metamorphism of the eucrite clasts. As discussed previously, Mayne et al. (2010) observed that eucrites, which were equilibrated with respect to their major element pyroxene composition, still showed zonation in their minor elements (Al, Cr, Ti) and a range of anorthite content within plagioclase. This indicates that major element pyroxene composition is not the best tool for assessing equilibration. The major elements of pyroxene equilibrate first when a eucrite is thermally metamorphosed, followed by plagioclase zonation (Table 4) and then by pyroxene minor element composition (Mayne et al., 2010).

These three criteria, major and minor elements in pyroxene and range of anorthite content in plagioclase, as well as textural data, were used to assess the relative equilibration for the eight eucrite clasts in this study. First I will describe the overall trends, then I will describe each sample in detail, with a chart summarizing their relative equilibration (Table 5).

Texture and Mineralogy

The eight eucrite clasts (listed in Table 3) exhibit a variety of textures, from ophitic and quenched, to skeletal and zoned grains, equigranular clasts, and laths (Appendix A1-H1). Mineral maps, elemental X-ray maps and BSE images (as discussed in 'Methodology') were used to help distinguish minerals and their textures.

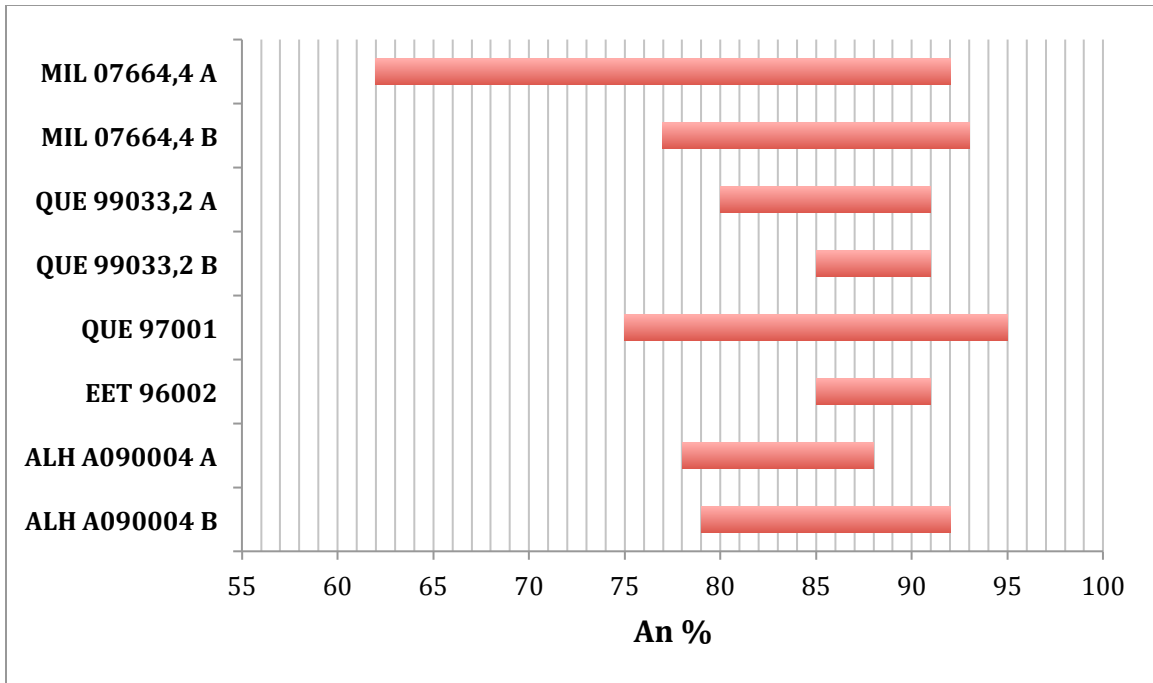


Table 4: Range of anorthite content present in the plagioclase data.

Clast	Major (Px)	Minor (Px)	Anorthite Equilibration	Texture	Overall Equilibration
MIL 07664,4 A	No	No	No	Plagioclase anhedral grains and small skeletal laths; zoned and quenched pyroxenes; groundmass made up of fine-grained plagioclase and pyroxene; silica and opaque phases present (sulfides and chromite).	Unequilibrated
MIL 07664,4 B	No	No	No	Zoned, skeletal pyroxene laths; matrix is quenched pyroxene and plagioclase; two anhedral plagioclase grains; opaque phases (sulfides).	Unequilibrated
QUE 99033,2 A	No	No	No	Ophitic texture with plagioclase laths of roughly equal size; matrix of zoned low-Ca pyroxene with high-Ca rims; silica and opaque phases (sulfides, chromite, ilmenite and FeNi metal).	Unequilibrated
QUE 99033,2 B	Yes	No	No	Sub-millimeter scale, equigranular plagioclase and pyroxene; pyroxene lamellae from exsolution; groundmass is pyroxene; opaque phases (ilmenite, sulfides, and chromite)	Partially Equilibrated
QUE 97001	No	No	No	Pyroxene laths, zoned and skeletal; laths with distinct low-Ca cores and high-Ca pyroxene rims; matrix is vitrophyric, silica-enriched plagioclase composition glass; silica and opaque phases (sulfides, chromite, possible FeNi metal)	Unequilibrated
EET 96002	Yes	No	No	Plagioclase laths; some pyroxene grains display fine lamellae from exsolution; silica and opaque phases (ilmenite, chromite, possible sulfides)	Partially Equilibrated
ALH 090004 A	No	No	No	Plagioclase laths; pyroxene grains that are slightly zoned with some areas of pyroxene groundmass; silica and opaque phases (sulfides, chromite, and ilmenite).	Unequilibrated
ALH 090004 B	No	No	No	Lath-like plagioclase grains; zoned pyroxenes and groundmass of pyroxene; silica and opaque phases (ilmenite and sulfides)	Unequilibrated

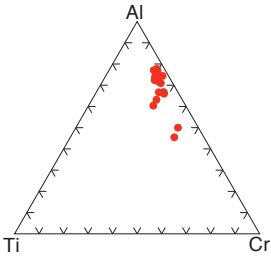
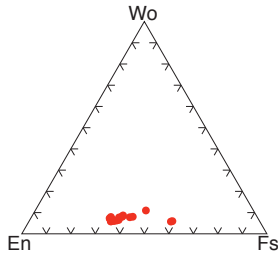
Table 5: Degree of equilibration for major and minor elements in pyroxene (Px), textural properties, and anorthite equilibration (less than 5mol%) for each of the eucrite clasts.

Each clast consists predominantly of pyroxene and plagioclase. QUE 99033,2B and EET 96002 contain both high- and low-Ca pyroxene as a result of exsolution, whereas all other samples had zoned pyroxenes. QUE 97001 was the only eucrite clast that did not contain plagioclase, but instead had glass with a silica-enriched plagioclase composition. Silica (seen as black in the SEM mineral maps) is observed in MIL 07664,4A, QUE 99033,2A, QUE 99033,2B, QUE 97001, EET 96002, ALH 090004A and ALH 090004B (Appendix: B1, C1, F1, G1, H1). However, the type of silica (quartz, tridymite, or cristobalite) was not determined in this study. Opaque phases were seen in all samples including ilmenite, chromite, troilite, other sulfides, and FeNi metal.

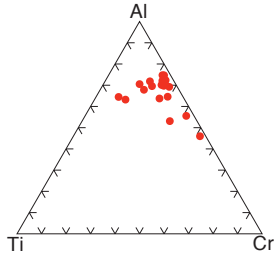
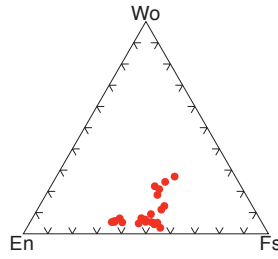
Mineral chemistry

Compositional data for pyroxene are shown in Fig. 16 with major element (Fe, Ca, Mg) and with minor element (Cr, Al, Ti) diagrams for each sample. Pyroxene compositions are in the range $En_{24-66}Fs_{21-60}Wo_{2-47}$. Plagioclase compositions fall in the range $An_{62-95}, Ab_{1-28}, Or_{0.1-16}$. The range in An content in each sample is shown in Table 4. We also used a Fe/Mg versus Fe/Mn ratio plot to show that all samples examined in this study were in fact eucrites (Fig. 17). These ratios are used to determine if samples have the same planetary origin (Papike et al., 2003) because their values are believed to remain constant during igneous processes. The plot shows that all of the samples lie within the same range. We compared this to other eucrite Fe/Mg versus Fe/Mn trends (Fig. 17), and found that they were similar. (Mittlefehldt and Lindstrom, 2003; Mayne et al., 2010).

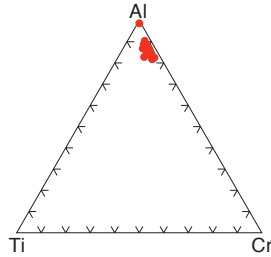
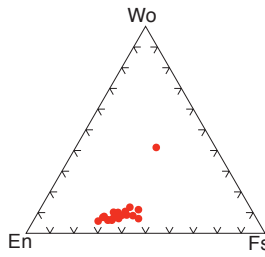
MIL 07664,4 A



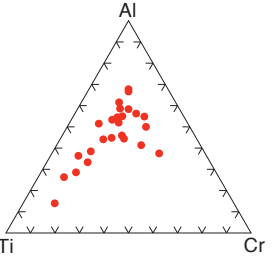
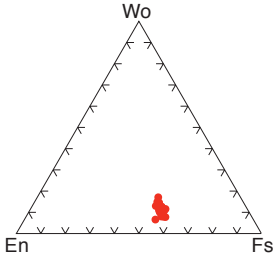
QUE 99033,2 A



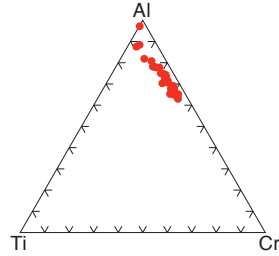
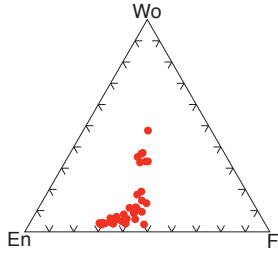
MIL 07664,4 B



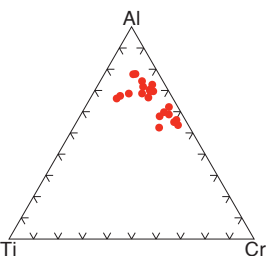
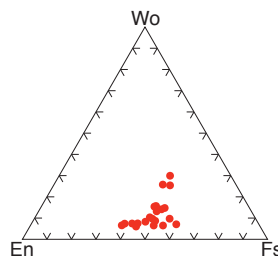
QUE 99033,2 B



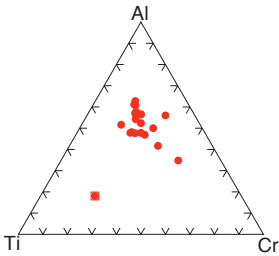
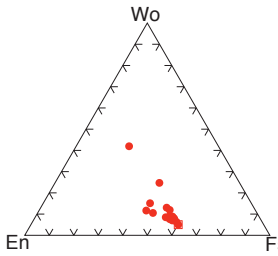
QUE 97001



ALH A090004 A



EET 96002



ALH A090004 B

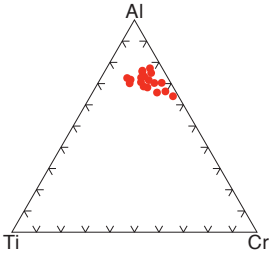
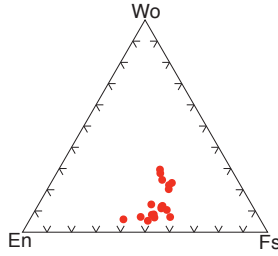


Figure 16: Microprobe data for pyroxenes in eucrite clasts. End-member pyroxene components on the left (Fs, En, Wo); minor elements on the right (Cr, Al, Ti).

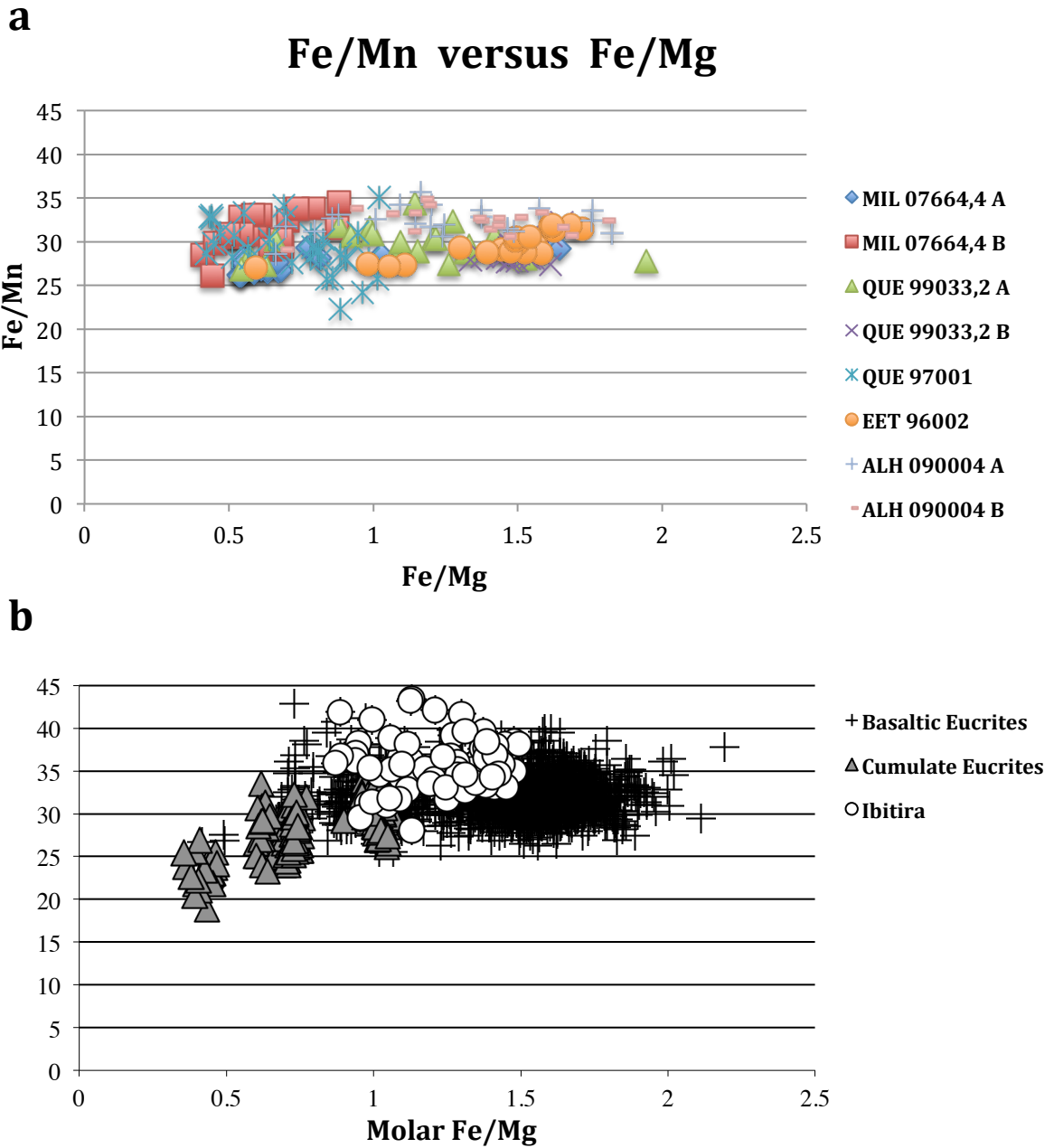


Figure 17: Fe/Mn versus Fe/Mg plot for eucrites in this study (a). Known eucrites (cross-symbol) in a Fe/Mn versus Fe/Mg plot (b) (Mayne et al., 2009).

Equilibration

After looking at the major and minor elements in pyroxene and range of anorthite content in each sample, all eucrite clasts were found to be unequilibrated, with the exception of two samples (QUE 99033,2B and EET 96002) having equilibrated major elements.

MIL 07664,4A

Texture and Mineralogy

MIL 07664,4A is a clast up to 2mm at its widest point, predominantly made up of pyroxene and plagioclase. Pyroxene is observed as larger zoned grains (up to 0.5mm in length) and smaller quenched crystals (Appendix A1). Plagioclase appears as larger, anhedral grains, of similar size to the large pyroxenes, and also as small, skeletal laths. The BSE image (Appendix A8) shows that fine-grained pyroxene and plagioclase make up the groundmass in this clast, along with opaque phases (Appendix A8). Opaque phases include several sulfide grains (~150µm wide), chromite (one grain ~20µm wide), as well as silica (the type of which has not been determined). Mesostasis appears in this clast, representing the last of the crystallizing melt. It is rich in late-stage phases, such as silica and opaque minerals (Mayne et al., 2009).

Mineral Chemistry

Pyroxene composition is in the range $En_{35-60}Fs_{32-57}Wo_{5-10}$. The elemental X-ray maps, the SEM map, and BSE image all show the pyroxene zonation (Appendix A1, A2, A8). The absence of high-Ca pyroxene analyses is attributed to the difficulty in sampling

such fine-grained crystals. In order to get an accurate measurement from the electron microprobe, we had to focus the microprobe beam in the middle of a pyroxene grain to achieve an analysis of only the pyroxene, with no input from the surrounding groundmass. MIL 07664,4A appears to follow the (Mg-Fe-Ca) trend “a” (Fig. 8a, Fig. 16) and is unequilibrated. The (Mg-Fe-Ca) trend depicts eucrite pyroxenes that start out Mg-rich, progressively become more Fe-rich, and finally more Ca-rich. However, after looking at the elemental X-ray maps further, one pyroxene grain can be observed with an Fe-rich core, and a more Mg-rich rim. This is the opposite trend expected for crystallizing pyroxenes (Mg-rich cores and Fe-rich rims). Minor element compositions cluster more toward the Al-rich end member (Fig 8d, Fig. 16). Plagioclase in MIL 07664,4A falls in the range $An_{79-92} Ab_{7-19} Or_{0.19-1}$ (Table 4). With a range in anorthite content of An_{79-92} , this clast has the largest An range of all eucrite clasts sampled.

Equilibration

Judging from the pyroxene zonation, major and minor elements and plagioclase data, in concordance with the three components used in Mayne et al. (2010), MIL 07664,4A is considered unequilibrated.

MIL 07664,4B

Texture and Mineralogy

MIL 07664,4B contains predominantly skeletal, zoned pyroxene laths up to 0.75mm in length (Appendix B1). Two anhedral plagioclase grains were seen in the BSE image (the larger being $\sim 100\mu\text{m}$ wide). The rest of the eucrite clast was extremely fine-grained and quenched, making it difficult to recognize mineral phases. However, BSE

images and elemental X-ray maps allowed for us to better resolve the mineralogy and textures. The quenched groundmass consisted of pyroxene and plagioclase. Opaque phases can be seen using the BSE image (Appendix B8) and Fe elemental X-ray map (Appendix B2); however, the grains were too small for detailed microprobe analysis. We used our knowledge of which opaque phases we would expect to see in eucrites, and what to look for in elemental X-ray maps and BSE images to identify them. Eucrites can contain ilmenite, chromite, FeNi metal, and sulfides (Mayne et al., 2009). Ti and Cr elemental X-ray maps can be used to identify ilmenite and chromite; however, in this sample the X-ray maps were not of sufficient resolution to determine these minerals. Sulfides were clearly seen from the S elemental X-ray map (Appendix B2).

Mineral Chemistry

MIL 07664,4B pyroxene compositions have a range of $\text{En}_{47-66} \text{Fs}_{27-43} \text{Wo}_{5-41}$ (Fig. 16). The zoned pyroxenes have Mg- and Fe-rich, Ca-poor cores, with increasing Ca towards the rim (Appendix B1). Only one analysis of high-Ca pyroxene was taken due to the extremely fine-grained nature of the clast. Difficulty in obtaining more high-Ca pyroxene analyses is described above in *MIL 07664,4A* on page 43. MIL 07664,4B pyroxene data exhibit the (Mg-Fe-Ca) trend (Fig. 8a, Fig. 16). This is confirmed by the elemental X-ray maps, which show a Ca-rich rim around pyroxene laths in this sample. The minor element compositions for pyroxene (Cr, Al, Ti) show a close clustering towards the Al-rich end member (Fig. 16). Plagioclase data shows a range of $\text{An}_{77-98} \text{Ab}_{1-20} \text{Or}_{0.10-1}$ (Table 4).

Equilibration

With respect to the three components defined by Mayne et al. (2010), this clast is considered unequilibrated. Initially, the fact that the minor element data cluster together might lead us to conclude this is an equilibrated trend, despite the major element data not being equilibrated. However, during metamorphism, major elements within pyroxenes equilibrate before minor elements, making it implausible that this clast would be equilibrated with respect to its minor elements only. Therefore, the minor elements must have crystallized with a narrow range of composition. Since the cluster is close to the Al-rich end member, it suggests that pyroxene was crystallizing from the melt just before plagioclase; we see plagioclase crystallization from the melt with a transition from Al-rich to more Ti-rich trends on the minor element ternary diagram (Fig. 16).

QUE 99033,2A

Texture and Mineralogy

QUE 99033,2 A is a clast that is 3.5mm in diameter, with an ophitic texture shown by pyroxene and plagioclase, both roughly 0.25mm in size (Appendix C1). The pyroxene in this sample is present in the groundmass as well as larger grains enclosing plagioclase. The larger grains have low-Ca cores with high-Ca rims. Plagioclase grains in this clast are laths, with the largest being 3.5mm in length. Opaque phases seen from the elemental X-ray maps include sulfides, chromite, ilmenite, and small areas of FeNi metal (Appendix C2). The reason we can identify FeNi metal without analyzing Ni for this clast is that in some opaque Fe-rich regions, Ti, Cr, and S were not abundant. Many

opaque grains were large, and the largest sulfide grain is $\sim 100\mu\text{m}$. Silica is also present, and although it was difficult to tell in this sample, it looks as if it is present in the mesostasis. The specific type of silica is not identified in this study.

Mineral Chemistry

Pyroxene compositions show a range of $\text{En}_{24-59}\text{Fs}_{33-54}\text{Wo}_{2-26}$ (Fig. 16). After looking at the zonation of QUE 99033,2A and the pyroxene composition ranges, these pyroxenes best fit trend “b” (Mg-Fe) (Fig. 8b, Fig. 16). This trend shows an Fe enrichment, as it does not trend solely towards the Ca-rich end member, as trend “a” does, but starts to trend more towards the Fe-rich end member. Minor elements show a trend toward the Al-rich end member, but also spread toward more Ti-rich compositions (Fig. 16). This suggests that the minor elements crystallized around the time plagioclase started to form. Plagioclase composition has a range of $\text{An}_{80-91}\text{Ab}_{7-18}\text{Or}_{0.19-0.88}$ (Table 4).

Equilibration

QUE 99033,2A is considered unequilibrated with respect to its major and minor elements in pyroxene and with the anorthite range being more than 5mol%.

QUE 99033,2B

Texture and Mineralogy

QUE 99033,2B is very fine-grained clast that contains sub-millimeter scale, anhedral, equigranular plagioclase and pyroxene (up to $\sim 100\mu\text{m}$ wide) (Appendix D1). Exsolution lamellae are present within the pyroxene (Appendix D9). This is caused by the exsolution of high-Ca augite from low- Ca pigeonite, which suggests that this clast

cooled slower than other clasts. In order to have a fine-grained texture and exhibit exsolution, QUE 99033,2B must have cooled quickly and be metamorphosed later, causing the pyroxene to equilibrate. Opaque phases include ilmenite, sulfides and chromite (Appendix D2). Fine-grained ilmenite is seen disseminated throughout the clast. Silica is also present. Compared to all other clasts, this is the only very fine-grained, equigranular clast, and probably has the smallest modal abundance of opaque phases.

Mineral Chemistry

Pyroxene composition in QUE 99033,2B shows the least variation of all the clasts ($\text{En}_{33-39} \text{Fs}_{49-56} \text{Wo}_{7-17}$), as seen from the cluster of data points (Fig. 16). The narrow range in the major elements of pyroxene and the presence of lamellae suggests that QUE 99033,2B exhibits trend “c” (Fig. 8c). Trend “c” (Fe-Ca) is an equilibrated trend, which geochemically shows the exsolution of high-Ca augite from low-Ca pigeonite. In Fig. 8c, trend “c” starts off Fe-rich and becomes progressively more Ca-rich. However, we have not analyzed high-Ca pyroxene in this sample. The absence of high-Ca pyroxene analyses is attributed to the difficulty in sampling such small grains, as described above on page 43. The minor elements show a large range in composition, from more Cr-rich to Al-rich to more Ti-rich (Fig. 16). This suggests that pyroxene was forming before, during, and after plagioclase crystallization. Plagioclase has range of $\text{An}_{85-91} \text{Ab}_{8-12} \text{Or}_{0.19-0.39}$ (Table 4). The anorthite content range is the smallest of all the samples, except EET 96002 (which has the same range).

Equilibration

QUE 99033,2B is equilibrated with respect to the major elements and shows exsolution lamellae. The spread in both the minor elements of pyroxene and An content indicate that this clast is not fully equilibrated. Minor element data show that it comes from an evolved melt, as seen from the Ti-rich trend. The texture is almost granoblastic, which means it looks more metamorphic than igneous. Fig. 18 compares QUE 99033,2 B to a granoblastic sample, Ibitira, from Mayne et al. (2010). While the minor element and plagioclase data suggest that it is unequilibrated, this clast is at least partially equilibrated, due to the equilibrated major elements and evidence of exsolution lamellae, as well as the granoblastic texture.

QUE 97001

Texture and Mineralogy

QUE 97001 is vitrophyric and is the largest clast in this study at 4.25mm in diameter (Appendix E1). The groundmass is quenched, suggesting this eucrite clast cooled very quickly. Pyroxene skeletal laths and grains dominate the clast, with some laths up to 1mm in length. Pyroxenes are zoned, as seen from the SEM and BSE images (Appendix E8). Mesostasis is present, and within it elemental X-ray maps were able to identify opaque phases and silica (Appendix E2). Opaque phases include sulfides, chromite, and possible FeNi metal. There are also sub-microscopic opaque phases spread through the quenched groundmass. Plagioclase is not present in this sample; however, the quenched groundmass is composed of glass with a silica-enriched plagioclase composition.

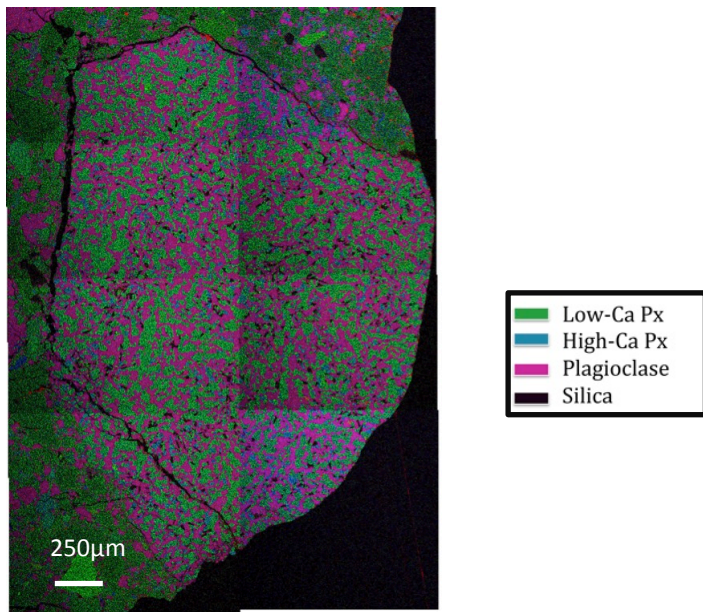
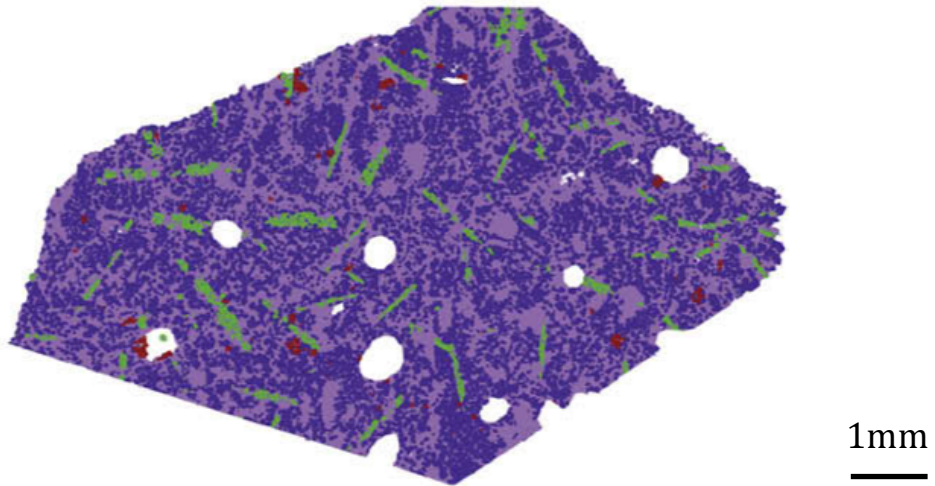


Figure 18: Comparison of Ibitira (left), which is granoblastic (adapted from Mayne et al., 2009), and QUE 99033,2B (right) which appears almost granoblastic. The Ibitira map shows blue-purple as pyroxene, lilac as plagioclase, green as silica, and red as oxides, sulfides, and metal.

Mineral Chemistry

Pyroxene data fall in the range $\text{En}_{25-61} \text{Fs}_{26-42} \text{Wo}_{3-47}$ (Fig. 16). Zonation is distinct, with low-Ca cores and high-Ca rims. QUE 97001 appears to follow the (Mg-Fe-Ca) trend (Fig.8a, Fig. 16), and is unequilibrated. Minor elements trend toward the Al-rich end member (Fig. 16). The groundmass is a glass with a silica-enriched plagioclase composition. This is reflected in the microprobe data (Appendix E6), which show that SiO_2 for QUE 97001 “plagioclase” ranges up to 72.5%, while in all other samples, SiO_2 in plagioclase ranges from ~40-50%. Since the glass with a silica-enriched plagioclase composition is not exactly plagioclase, we have excluded it from Table 4.

Equilibration

This sample is unequilibrated with respect to the three components described by Mayne et al., (2010),

EET 96002

Texture and Mineralogy

EET 96002 has subophitic texture and is one of the smaller eucrite clasts (1.75mm in diameter). It is the coarsest clast in this study (Appendix F1). Plagioclase occurs in large laths up to 0.6mm in length. Pyroxene is present as large anhedral grains that exhibits exsolution lamellae (Appendix F9), like QUE 99033,2 B. This is evidence that this clast cooled slowly. Abundant mesostasis hosts silica and opaque phases (Appendix F2). Opaque phases include ilmenite, chromite (one grain up to ~20 μm), and possible sulfides (data quality makes it difficult to identify distinct grains).

Mineral Chemistry

Pyroxene composition shows a range of $\text{En}_{32-44} \text{Fs}_{21-60} \text{Wo}_{5-41}$ (Fig. 16). EET 96002 exhibits pyroxene crystallization trend “c” (Fig. 8c, Fig. 16). Minor element data show a wide range, mostly grouping around the Al-rich end member, with one point near the Ti-rich end member (Fig. 16). Plagioclase range is $\text{An}_{85-91} \text{Ab}_{8-14} \text{Or}_{0.19-0.49}$, with the anorthite range being the smallest of all samples, besides QUE 99033,2 B (Table 4).

Equilibration

EET 96002 is equilibrated with respect to the major elements, although minor elements and plagioclase data show that it is unequilibrated. In contrast with the other sample that shows exsolution lamellae, EET 96002 maintains its igneous texture.

ALH 090004A

Texture and Mineralogy

ALH 090004A is a coarse-grained clast that is ~2.5mm at its widest point (Appendix G1). Pyroxene grains are zoned, as shown by the BSE image (Appendix G8) and up to 0.5mm in size. Plagioclase occurs in the form of large laths (up to ~0.5mm in length). The mesostasis hosts silica and opaque phases (Appendix G2). Opaque phases include fine-grained sulfides, chromite, and ilmenite (up to ~20 μm across).

Mineral Chemistry

Pyroxene composition is in the range $\text{En}_{24-56} \text{Fs}_{37-55} \text{Wo}_{6-29}$ (Fig. 16). Major element data and evidence of pyroxene zonation suggest that ALH 090004A exhibits trend “a” (Mg-Fe-Ca) (Fig. 8a, Fig. 16). Minor element data show a trend towards the Al-

rich end member, suggesting the pyroxene crystallized before plagioclase formation (Fig. 16). Plagioclase shows a range of $An_{78-86} Ab_{12-20} Or_{0.29-1}$ (Table 4).

Equilibration

This sample is considered unequilibrated with respect to the major and minor elements of pyroxene, as well as the anorthite content range.

ALH 090004B

Texture and Mineralogy

ALH 090004B is a coarse-grained clast up to 1.3mm at its widest point (Appendix H1). Pyroxene grains range up to 0.4mm wide and BSE images show that they are slightly zoned (Appendix H8). Plagioclase grains are up to ~0.5mm in length, and are not lath-like, as was the case with ALH 090004A. As with most of the clasts, ALH 090004B has mesostasis containing silica and some opaque phases. Judging from the data, ALH 090004A has a similar mineral chemistry and texture to ALH 090004B. In contrast to ALH 090004A, this clast does not have chromite, but does have ilmenite and sulfides present (Appendix H2).

Mineral Chemistry

Pyroxene compositions show a range of $En_{27-55} Fs_{38-56} Wo_{5-29}$ (Fig. 16). ALH 090004B exhibits trend “a” (Mg-Fe-Ca) (Fig. 8a, Fig. 16). The major element pyroxene trends look very similar to those in ALH 090004A. Minor element data seem to cluster towards the Al-rich end member (Fig. 16). This represents pyroxene crystallizing in a narrow range in the melt before plagioclase started to form. Plagioclase data show a range of $An_{79-91} Ab_{7-19} Or_{0.19-0.97}$.

Equilibration

ALH 090004B is considered unequilibrated with respect to the three components used in this study. Although minor element data were clustered, we know that during metamorphism, major elements of pyroxene equilibrate before minor elements. Therefore, the minor elements in this case probably crystallized in a narrow range just as plagioclase was forming. This is also the case for MIL 07664,4B. The range in anorthite content is greater than 5mol%, thus making it unequilibrated (Table 4).

Discussion

Implications for Vesta and Fine-grained Eucrites Using ALH A81001

Early in Solar System history, Vesta differentiated into a core-mantle-crust structure, with eucrites making up the upper portion of the crust. After differentiation, Vesta is believed to have experienced a global metamorphic event due to the large number of eucrites that have been re-equilibrated by thermal metamorphism (Yamaguchi et al., 1997). Unlike the rest of the eucrite-only collection, most of the fine-grained eucrite clasts examined in this study preserve their original compositional zonation; they are unequilibrated eucrites. ALH A81001, which was studied by Mayne et al. (2010), is one of the few fine-grained, partially unequilibrated eucrites in the eucrite-only collection. While ALH A81001 is equilibrated with respect to the major elements in pyroxene (Fig. 8c), the minor elements are unequilibrated. As discussed previously, not only does ALH A81001 preserve its original minor element pyroxene crystallization trends, the pyroxenes it contains are also Cr-rich. This is significant, because, as previously mentioned in *'Thermal metamorphism in eucrites'*, Cr-rich eucrite pyroxenes crystallize from a primitive melt. Therefore, ALH A81001 must have formed from a primitive melt that was not subject to the global metamorphic event that occurred on Vesta. Mayne et al. (2010) showed that this eucrite could be used to test the formation models for Vesta, because it could only be formed in very specific environments in each of the proposed models.

The magma ocean theory states that while Vesta was still in a molten state, convection kept crystallized magma from sinking into a cumulate pile, and equilibrium

crystallization began. With increasing crystallization, convection ceased and the crystals and melt started to segregate, leaving behind residual magmas (Righter and Drake, 1997). In this environment, Mayne et al. (2010) suggested that ALH A81001 could only have formed as a quench crust, as Cr-rich pyroxenes would have crystallized early from the magma ocean. Most early-crystallized pyroxenes would have settled to the bottom of the magma ocean as slow-cooled, cumulate samples, unless they were part of the quench crust. If this theory is correct, ALH A81001-like eucrites would be abundant (Mayne et al., 2010), global-scale units.

The partial melting model involves a single source region with primary magmas produced by different degrees of partial melting (Stolper, 1977). It is suggested that global metamorphism occurred by successive lava flows being erupted on top of older flows, eventually reaching a thickness that produced metamorphic temperatures at depth, so as to ultimately equilibrate the eucrites (Yamaguchi et al., 1996; Mayne et al., 2010). In the partial melting model, ALH A81001 could have formed as a late-stage partial melt of a primitive source region. Such units would likely be small, localized units and we would not expect ALH A81001-like eucrites to be abundant.

In our examination of the howardite collection at the Smithsonian, we only identified eight fine-grained clasts that appeared similar to ALH A81001. We can, therefore, conclude that fine-grained eucrites are not abundant in either the howardite or eucrite collection. This, in turn, suggests that fine-grained eucrites are not common on the surface of Vesta. This does not support the magma ocean theory, because in this model, fine-grained eucrites would have to represent a global or near global unit.

Comparisons of Samples with Two Clasts

Three of the thin sections studied, MIL 07664,4, QUE 99033, and ALH 090004, contain two different fine-grained eucrite clasts. MIL 07664,4 A and B are only 2.5mm away from each other (Appendix A7, B7) but there are significant differences between them (Table 3 and Fig. 18). Clast “A” (Appendix A1) is a bigger clast that contains large plagioclase laths and granular pyroxene; conversely clast “B” (Appendix B1) contains pyroxene laths and plagioclase in a quenched matrix of high- and low-Ca pyroxene and plagioclase. Major element data for pyroxene in these clasts appear similar, although no high-Ca pyroxene data were collected (see MIL 07664,4A descriptions page 42 for explanation). Pyroxene minor element data show that “A” is unequilibrated with respect to the minor elements of pyroxene, but clast “B” appears equilibrated. However, minor elements do not equilibrate before major elements, as noted previously on pg. 47 (Mayne et al., 2010; Pun and Papike, 1996). The minor elements in clast “B” are most likely exhibiting their original crystallization trend, suggesting pyroxene crystallized with a narrow compositional range in minor elements, likely at the time of plagioclase formation.

QUE 99033,2 A and B (Appendix C1, D2) display very different compositions and textures despite being about a millimeter apart (Appendix C7, D7). Clast “A” is coarser grained with an ophitic texture, while clast “B” is finer grained and equigranular. Major and minor element data for pyroxenes (Fig. 16) clearly illustrate that clast “A” is unequilibrated; however, clast “B” is equilibrated with respect to the major elements for pyroxene. This is confirmed by the presence of pyroxene exsolution lamellae. This suggests that QUE 99033,2B may have been subject to slight metamorphism. Unlike the

other thin sections with multiple clasts, ALH 090004 A and B (Appendix G1, H1) are texturally and compositionally the most alike. Clast “A” is the larger of the two clasts and contains pyroxene grains and plagioclase laths, while clast “B” has primarily anhedral plagioclase grains. Both clasts contain zoned pyroxenes and granular pyroxene. Major element data for pyroxene are very similar (Fig. 16); however the minor element data for pyroxene show slight differences. Clast “A” exhibits a larger range in composition, while the data for clast “B” are loosely clustered together, suggesting that, as with MIL 07664,4 B, the pyroxenes crystallized with a narrow compositional range. The range in An content also is similar, although not identical. It seems possible that ALH 090004A and ALH 090004B are originally from the same eucrite unit on the surface of Vesta.

While ALH 090004A and B are similar, the “A” and “B” clasts within both MIL 07664,4 and QUE 99033,2 are different both texturally and compositionally. This strongly suggests that these eucrite clasts are from different geologic units on the surface of Vesta. The variety of clasts found within the howardites as a whole suggests that individual howardites reflect the local geology of their source region, as opposed to a globally homogenized surface on Vesta. MIL 07664,4 and QUE 99033,2 contain two very different eucrite clasts in a thin section that is only one inch in diameter (2.5cm). If, as suggested, howardites do reflect local geology, this would imply that fine-grained eucrites exist as small-scale, localized units on the surface of Vesta. The formation of such eucrites is best attributed to partial melting.

The formation of these eucrite clasts can be easily explained within the partial melting model. They likely represent a series of small-scale partial melts that formed late in Vesta's history. Their late formation allowed them to escape the metamorphic equilibration event experienced by most eucrites. The fine-grained eucrites show compositional variations that indicate they crystallized from melts with varying degrees of evolution (from Cr-rich, primitive ALH A81001 to the more Ti-rich, evolved clast QUE 99033,2B). This suggests that the surface of Vesta has a complex geologic history. This is supported by the initial data returned by the Dawn spacecraft, which suggest that it "has striking diversity in its composition" (GSA Press Release, 2011) (Fig. 19).

Unique Eucrite Clasts

The clasts examined in this study are unique in several ways. I will discuss a rare pyroxene grain discovered in MIL 07664,4A, before commenting on the importance of these clasts and how they enhance our knowledge of the eucrites as a whole.

Reverse Zonation

When looking at MIL 07664,4A, one large pyroxene grain was observed to have reverse zonation (Fe-rich core, Mg-rich rim). As pyroxenes crystallize from a magma, they become progressively more Fe-rich (or Mg-poor). The grain in MIL 07664,4A (Fig. 20) has an Fe-rich core that becomes progressively more Mg-rich towards the rim. The very outer rim of this grain then exhibits more normal zonation with a thin, more Fe-rich rim. This reverse zonation has only been identified in a few other HED samples (Schwartz and McCallum, 2005) and has, in one case, been attributed to metasomatism

(Mittlefehldt pers. comm.). MIL 07664,4A is an unequilibrated eucrite that has not undergone metasomatism and so alternative explanations must be sought.

Hewins (1974) described a scenario in which low-Ca pyroxenes with Mg-rich rims were attributed to increasing oxygen fugacity during crystallization. An increase of oxygen fugacity would initiate magnetite crystallization, enriching the magma in Mg relative to Fe. However, changing oxygen fugacity is inconsistent with theories for the petrogenesis of Vesta (Mittlefehldt and Lindstrom, 2003; Barrat et al., 2010). Indeed, as described earlier (page 9), oxygen isotopes are used in planetary science to identify if meteorites are from the same parent body. If oxygen fugacity were to vary during differentiation, then oxygen isotopes would vary for the HED meteorites, which is not observed.

Nakagawa and Wood (2002) propose an alternative theory that reverse zoning can form from magma mixing. In a low temperature, evolved magma, after crystallization of Fe-rich cores, an injection of a high temperature magma would cause Mg-rich pyroxene rims to crystallize around the cores. Nakagawa and Wood (2002) also mentioned that if there was just one injection of high-temperature magma, that it would have been cooled by the lower temperature magma; thus, continued intermittent injections might have been necessary for the growth of Mg-rims.



Figure 19: Dawn at Vesta (NASA/JPL-Caltech/ UCLA/MPS/DLR/IDA, 2011)

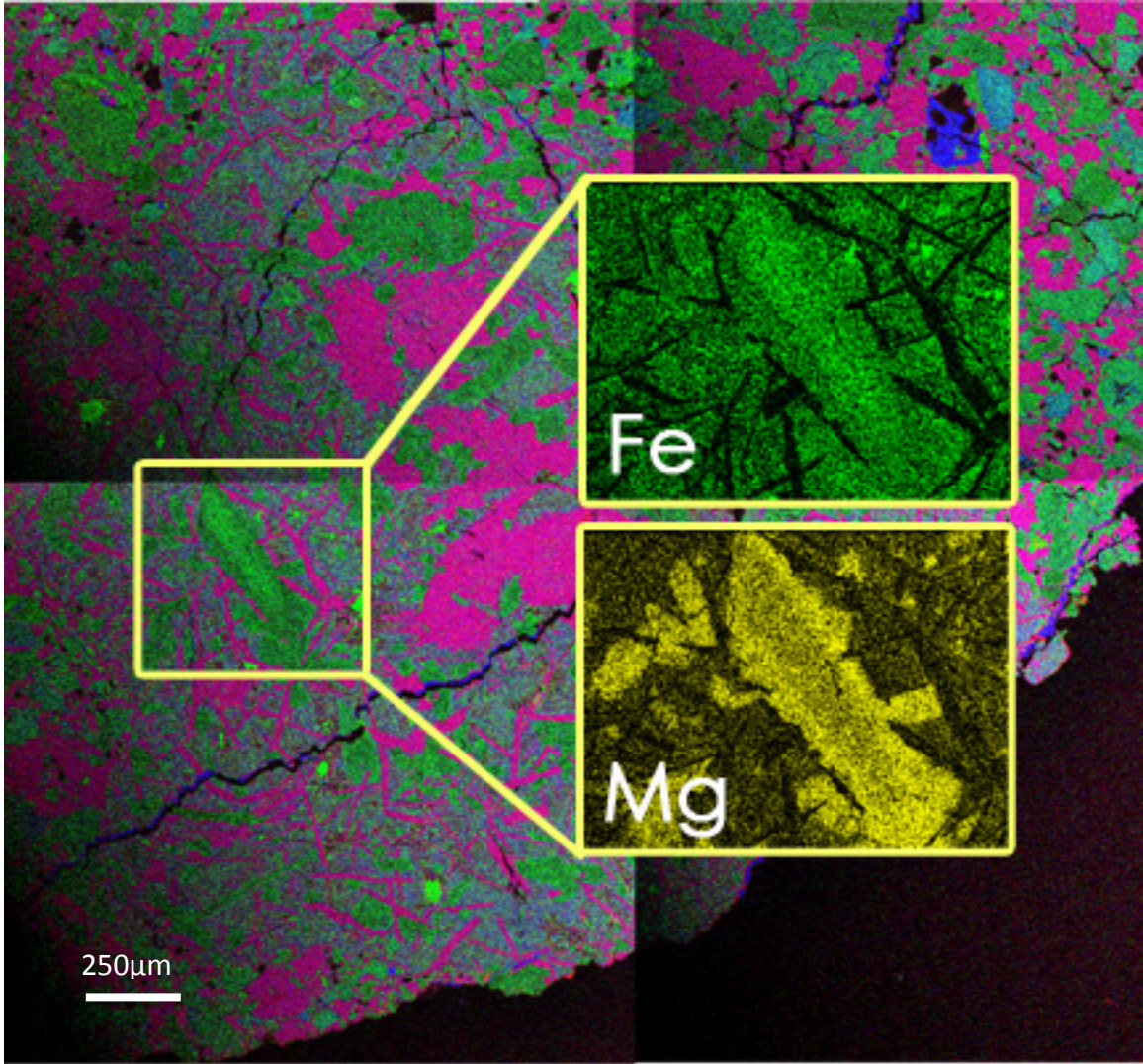


Figure 20: MIL 07664,4A pyroxene exhibiting reverse zoning with Fe-rich cores and an Mg-rich rim.

Expanding our Knowledge of Fine-grained Eucrites

Fine-grained eucrites are not common in the eucrite-only collection; therefore, these eight fine-grained eucrite clasts represent a significant addition to the fine-grained eucrite collection. More importantly, the eucrites studied here are unequilibrated, with the exception of QUE 99033,2B and EET 96002, which are equilibrated with respect to the major elements in pyroxene. This makes them extremely rare, as the majority of meteorites in the eucrite-only collection contain pyroxenes that have equilibrated major elements (Reid and Barnard, 1979), with around 50% of these also showing complete pyroxene equilibration (major and minor). Therefore, these clasts represent some of the most pristine eucrite samples discovered to date.

The minor element trends for the pyroxenes in the eucrites within this study vary from Al- to Ti-rich. If they are combined with the previously described Cr-rich ALH A81001, then we can conclude that eucrites exhibiting the complete range of minor element compositional zonation exist on the surface of Vesta. This tells us that the fine-grained eucrites crystallized from primitive, intermediate, and more evolved magmas.

The rarity of fine-grained, unequilibrated eucrites suggests that they represent small units on the surface of Vesta. This is supported by evidence previously discussed for the howardites that contain multiple clasts. The fact that the majority of fine-grained eucrites appear unequilibrated indicates that these were amongst the last flows to crystallize on the Vestan surface, allowing them to avoid the slow cooling and equilibration experienced by the earlier eucrites formed below them in the crust.

Conclusions

Vesta is a differentiated asteroid that has remained relatively unchanged since its formation in the early Solar System. Vesta is unique because it is the only asteroid for which we have an associated meteorite group, the HEDs. The petrogenesis of Vesta is not well understood, and currently both partial melting and magma ocean models are used to describe its formation. The work of Mayne et al. (2010) suggests that the abundance of fine-grained, unequilibrated eucrites may allow us to distinguish which of the models provides the best fit for Vesta's formation. In a magma ocean model, fine-grained unequilibrated eucrites would be abundant, whereas partial melting would produce only small amounts of such samples. We know that fine-grained eucrites are not common in the eucrite-only collection. In this study, we investigated the abundance of fine-grained eucrite clasts within the howardite member of the HEDs to better understand the formation of Vesta.

- All howardite thin-sections in the National Meteorite Collection at the Smithsonian Institution were examined. Out of over 200 samples, five howardites were identified to contain eight fine-grained eucrite clasts. If the HEDs accurately reflect the units on the surface of Vesta then fine-grained eucrites are not common. This does not fit with the magma ocean model for Vesta's petrogenesis. Instead it suggests a much more globally heterogeneous surface.

- The mineral chemistries and textures were analyzed for each of the eight clasts. None of the clasts were completely equilibrated and six of the clasts were fully unequilibrated with respect to all three components described by Mayne et al. (2009) to assess the thermal equilibration of eucrites. This makes these clasts a very rare data-set as the vast majority of all eucrites have experienced at least partial re-equilibration.
- Three of the thin-sections examined contained two different fine-grained eucrite clasts. The clasts found within MIL 07664,4 and QUE 99033,2 have different compositions and textures, suggesting that they are from different eucrite units on the surface of Vesta. If, as proposed, howardites reflect local geology (i.e. they contain clasts from units near to where they formed as opposed to clasts sourced from all over the asteroid's surface), then this would suggest that these fine-grained eucrites come from units with very limited extent on the surface of Vesta. Since there is such variety of clasts in the howardites with multiple eucrite clasts, we can conclude that the local geology on the surface of Vesta is very complex, suggesting that Vesta on a global scale would have an extremely wide variety of geologic units.
- MIL 07664,4A contains a rare pyroxene grain that exhibits reverse zoning (Fe-rich core to Mg-rich rim). This may be a result of magma mixing processes occurring during crustal formation on the asteroid Vesta.
- As stated previously, the eight eucrite clasts analyzed in this study represent a unique new data-set. They are unlike the rest of the eucrite collection because they are largely unequilibrated. Their mineral compositions reflect

crystallization from primitive, intermediate, and evolved magmas. These samples likely represent the last melts to form and crystallize on the surface of Vesta.

References

- Barrat J., Yamaguchi A., Brigitte Z., Bollinger C., and Bohn M. 2010. Relative chronology of crust formation on asteroid Vesta: Insights from the geochemistry of diogenites. *Geochimica et Cosmochimica Acta* 74:6218-6231.
- Binzel R. P, and Xu S. 1993. Chips off of asteroid 4 vesta: evidence for the parent body of basaltic achondrite meteorites. *Science* 260:186-191.
- Chamberlin, A. 2007. JPL/Caltech http://ssd.jpl.nasa.gov/?histo_a_ast
- Clayton R. N., and Mayeda T. K. 1996. Oxygen isotope studies of achondrites. *Geochimica et Cosmochimica Acta* 60:1999-2017.
- Drake J. D. 2001. The Eucrite/vesta story. *Meteoritics & Planetary Science* 36:501-513.
- Dumas C. Keck Observatory. 2011. NASA-JPL http://www.nasa.gov/mission_pages/dawn/ceresvesta/
- Geological Society of America, "NASA's Dawn Science Team Presents Early Science Results," news release. October 12, 2011.
- Hewins R. H. 1974. Pyroxene crystallization trends and contrasting augite zoning in the Sudbury nickel irruptive. *American Mineralogist* 59:120-126.
- Keil K. 2002. Geological History of Asteroid 4 Vesta: The "Smallest" Terrestrial Planet. *Asteroids iii*, edited by Bottke W.F., Cellino A., Paolicchi P., and Binzel R.P. Tuscon: University of Arizona Press. 573-584 p.
- Kleine T., Münker C., Mezger K., and Palme H. 2002. Rapid accretion and early core formation on asteroids and the terrestrial planets from Hf-W chronometry. *Nature*. 418:952-955.
- Mason B. 1962. *Meteorites*. New York: John Wiley and Sons.
- Mayne R. G., McSween H. Y., McCoy T. J., and Gale A. 2009. Petrology of the unbrecciated eucrites. *Geochimica et Cosmochimica Acta* 73:794-819.
- Mayne R. G, Sunshine J. M, McSween H. Y, McCoy T. J, Corrigan, C. M, and Gale A. 2010. Petrologic insights from the spectra of the unbrecciated eucrites: implications for Vesta and basaltic asteroids. *Meteoritics & Planetary Science* 45:1074–1092.
- McCord T. B., Adams J. B., and Johnson T. V. 1970. Asteroid Vesta: spectral reflectivity and compositional implications. *Science* 168:445-1447.
- McSween H. Y. 1999. *Meteorites and their parent planets*. New York: Cambridge University Press.
- Meteoritical Bulletin Database. <http://tin.er.usgs.gov/meteor/metbull.php>

- Miller R. 2008. <http://www.black-cat-studios.com/catalog/asteroids2.html>
- Mittlefehldt D. W., and Lindstrom M. M. 2003. Geochemistry of eucrites: Genesis of basaltic eucrites, Hf and Ta as petrogenetic indicators for altered Antarctic eucrites. *Geochimica et Cosmochimica Acta*. 67:1911-1935.
- Nakagawa K. W. and Wood C. P. 2002. Mixed magmas, mush chambers and eruption triggers: Evidence from zoned clinopyroxene phenocrysts in andesitic scoria from the 1995 eruptions of Ruapehu Volcano, New Zealand. *Journal of Petrology* 43:2279-2303.
- NASA. 2007, November 22
http://www.nasa.gov/mission_pages/dawn/ceresvesta/index.html
- NASA. 2009. <http://www.jpl.nasa.gov/education/images/pdf/ss-meteors.pdf>
- NASA. Vesta by Dawn. 2011. NASA/JPL-Caltech/ UCLA/MPS/DLR/IDA
http://dawn.jpl.nasa.gov/multimedia/vesta_dawn_gallery.asp
- O'Neill C. O., and Delaney J. S. 1982. Zoning of eucritic feldspars. *Meteoritics* 17:265.
- Papike J. J., Karner J. M., and Shearer C. K. 2003. Determination of planetary basalt parentage: a simple technique using the electron microprobe. *American Mineralogist* 88:469-472.
- Piazzi G. 1801. Risultati delle Osservazioni della Nuova Stella scoperta il dì 1. *Gennajo all'Osservatorio reale di Palermo*. Nella Reale Stamperia, Palermo. 25 p.
- Pun A. and Papike J.J. 1996. Unequilibrated eucrites and the equilibrated Juvinas eucrite: Pyroxene REE systematics and major, minor, and trace element zoning. *American Mineralogist* 81:1438-1451.
- Rayman M. D, Fraschetti T. C, Raymond C. A, and Russell C. T. 2006. Dawn: A mission in development for exploration of main belt asteroids Vesta and Ceres. *Acta Astronautica* 605:605-616.
- Reid A. M., and Barnard B. M. 1979. Unequilibrated and equilibrated eucrites. 10th Lunar and Planetary Science Conference 1019-1021p.
- Righter K. and Drake M. J. 1997. A magma ocean on Vesta: Core formation and petrogenesis of eucrites and diogenites. *Meteoritics & Planetary Science* 32:929-944.
- Righter K. and Garber J. 2011. <http://curator.jsc.nasa.gov/antmet/hed/index.cfm>
- Russell C. T., Coradini A., Feldman W. C., Jaumann R., Konopliv A. S., McCord T. B., McFadden L. A., McSween H. Y., Mottola S., Neukum G., Pieters C. M., Raymond C. A., Smith D. E., Sykes M. V., Williams B. G., and Zuber M. T. 2002. Dawn: a journey to the beginning of the solar system. *Proceedings of Asteroids, Comets, Meteors* 63-66 p.
- Russell C. T., Coradini A., Christensen U., De Sanctis M. C., Feldman W. C., Jaumann R., Keller H. U., Konopliv A. S., McCord T. B., McFadden L. A., McSween H. Y., Mttola S.,

- Neukum G., Pieters C. M., Prettyman T. H., Raymond C. A., Smith D. E., Sykes M. V., Williams B. G., Wise J., and Zuber M. T. 2004. Dawn: a journey in space and time. *Planetary and Space Science* 52:465-489.
- Russell C. T., Capaccioni F., Coradini A., Christensen U., De Sanctis M. C., Feldman W. C., Jaumann R., Keller H. U., Konopliv A., McCord T. B., McFadden L. A., McSween H. Y., Mottola S., Neukum G., Pieters C. M., Prettyman T. H., Raymond C. A., Smith D. E., Sykes M. V., Williams C. M., and Zuber M. T. 2006. Dawn discovery mission to Vesta and Ceres: present status. *Advances in Space Research* 38:2043-2048.
- Ruzicka A., Snyder G. A., and Taylor L.A. 1997. Vesta as the howardite, eucrite, and diogenite parent body: Implications for the size of a core and for large-scale differentiation. *Meteoritics & Planetary Science* 32:825-840.
- Schwartz J. M., and McCallum I. S. 2005. Comparative study of equilibrated and unequilibrated eucrites: Subsolvus thermal histories of Haraiya and Pasamonte. *American Mineralogist* 90:1871-1886.
- Serio G. F., Manara A., and Sicoli P. 2002. Giuseppe Piazzi and the discovery of Ceres. *Asteroids iii*, edited by Bottke W.F., Cellino A., Paolicchi P., and Binzel R.P. Tucson: University of Arizona Press 17-24 p.
- Stolper E. 1977. Experimental petrology of eucritic meteorites. *Geochim. Cosmochim. Acta* 41:587-611.
- Taylor G. J. 2009. PSRD: The complicated geologic history of asteroid 4Vesta. <http://www.psrh.hawaii.edu/June09/Vesta.granite-like.html>
- Thomas P. C., Binzel R. P., Gaffey M. J., Storrs A. D., Wells E., and Zellner B. H. 1997. Impact excavation on asteroid 4Vesta: Hubble space telescope results. *Science* 277:1492-1495.
- Wadhwa M., Srinivasan G., and Carlson R. W. 2006. Timescales of planetary differentiation in the early solar system. *Meteorites and the Early Solar System II* (eds. Lauretta D. S. and McSween H. Y. Jr.). Tucson: University of Arizona Press. 715-733 p.
- Wasson J. T. and Wetherill G. W. 1979. Dynamical, chemical and isotopic evidence regarding the formation locations of asteroids and meteorites. In *Asteroids* (T. Gehrels, ed.), pp. 926-974. Univ. of Arizona, Tucson.
- Yamaguchi A., Taylor G. J., and Keil K. 1996. Global crustal metamorphism of the eucrite parent body. *Icarus* 124:97-112.
- Yamaguchi A., Taylor G. J., and Keil K. 1997. Metamorphic history of the eucritic crust of 4 Vesta. *Journal of Geophysical Research* 102:13381-13386.

Vita

Personal Background	Samantha Elizabeth Smith Dallas, Texas Daughter of Gregory Steven and Janice Marie
Education	Diploma, Douglas MacArthur High School, San Antonio, Texas, 2005 Bachelor of Science, Geology, Texas A&M University – Corpus Christi, Corpus Christi, TX 2009 Master of Science, Geology, Texas Christian University, Fort Worth, TX 2011
Experience	Geotech, January 2008 – May 2009 Imagine Resources, LLC, Corpus Christi, TX Teaching Assistantship, August 2009 – December 2009 Texas A&M University – Corpus Christi, Corpus Christi, TX Research Assistantship, June 2010 – May 2011 Texas Christian University, Fort Worth, TX Gallery Assistant, August 2011 – December 2011 Oscar E. Monnig Meteorite Gallery (TCU), Fort Worth, TX Geologist/GIS Analyst, August 2011 - present Double Eagle Development, LLC, Fort Worth, TX
Professional Memberships	Meteoritical Society 2011-present

Abstract

USING PETROLOGY AND MINERALOGY TO UNDERSTAND THE SURFACE OF VESTA: A COLLECTION OF FINE-GRAINED EUCRITES

by Samantha Elizabeth Smith, M.S., 2012
School of Geology, Energy and the Environment
Texas Christian University

Thesis Advisor: Rhiannon G. Mayne, Assistant Professor of Geology

Fine-grained eucrites in howardites may help us understand the geologic history of the asteroid 4Vesta, as they represent the crustal material. Recent work by Mayne et al. (2010) suggests that fine-grained eucrites are not common in the eucrite collection alone and that eucrite clasts in howardites may show a greater variety. After looking at the entire US Antarctic and non-Antarctic howardite collection in the Smithsonian's Department of Mineral Sciences, five howardites were found to have eight fine-grained eucrite clasts within them, out of over 200 howardite samples. SEM mineral maps were used to identify textures and initial geochemistry, and electron microprobe data were obtained for detailed chemical analysis. Results show that even within a small group of fine-grained eucrites, the clasts have a great textural and compositional variety. This implies that geologic events on Vesta's crust were small-scale, localized and very complex.